ENHANCING METHANOL ELECTRO-OXIDATION BY DOUBLE OXIDE INCORPORATION WITH PLATINUM ON CARBON NANOTUBES

_____

A Thesis presented to the Faculty of the Graduate School at

the University of Missouri-Columbia

_____

In partial fulfillment of the Requirements for the Degree Master of Science

_____

by

AHMED MOHAMMED JASIM AL-KHAZRAJI

Dr.Yangchuan Xing, Thesis Supervisor

DECEMBER 2016

The undersigned, appointed by the dean of the Graduate School, have

examined the thesis entitled

ENHANCING METHANOL ELECTRO-OXIDATION BY DOUBLE

OXIDE INCORPORATION WITH PLATINUM ON CARBON

NANOTUBES

Presented by Ahmed Mohammed Jasim,

a candidate for the degree of Master of Science,

and hereby certify that, in their opinion, it is worthy of acceptance.

Professor Yangchuan Xing

Professor David G. Retzloff

Professor Matthew R. Maschmann

ACKNOWLEDGMENTS

TABLE OF CONTENT

LIST OF FIGURES

LIST OF TABLE

ABSTRACT

Electro-oxidation of methanol was investigated on platinum catalyst supported on a double oxide nanocomposite support of tin oxide and carbon-doped titanium dioxide. The Pt-SnO$_2$-C-/CNTs electro catalyst demonstrated about 20% and 44% percent higher forward peak current density than Pt-SnO$_2$/CNTs and E-TEK, respectively. The kinetics of formation of the oxygenated species (-OH) groups was dramatically enhanced upon doped titanium dioxide incorporation. This leads to a much lower onset potential of adsorbed CO oxidation. Doping by carbon in the titanium dioxide makes the oxide support electrically conductive.

Shifting in Pt oxidation state was noted, which refers to the influence of the metal oxide incorporation with platinum on the CNTs. The purpose of the coating is to avoid corrosion at high potentials and enhance the durability of the catalyst in an acidic medium. Therefore, the oxide coating was the key factor for the enhanced stability of the Pt catalyst and for the increase of current density during methanol electro-oxidation.

CHAPTER 1. Introduction

In 1839, William Robert Grove described the main principles of the fuel cell when he noticed the generation of electrical current from the reaction of oxygen and hydrogen in the presence of platinum in sulfuric acid. He called his observation a "gaseous voltaic battery" [1]. In 1889, the two chemists Ludwig Mond and Charles Lenger defined the term of "fuel cell" when they were attempting to design the first device by using the air and industrial coal gas. However, in the end of 1800s, and after the internal combustion engine was invented and the use of fossil fuels grew exponentially, the efforts on perfecting the fuel cell diminished.

Nevertheless, in today's world, due to environmental issues from oil burning and other pollutant sources, Proton Exchange Membrane (PEM) fuel cells, as clean, energy-converting devices have drawn a great deal of attention in the recent two decades due to their high energy density and negligible emissions [2]. PEM fuel cells have many remarkable application areas, including transportation, stationary and portable power, and micro-power. Since the 1960s, chemical engineers have done great and intensive work in the development of PEM fuel cells. People have started seeking other approaches that are environmentally-friendly and cost-effective. Direct methanol fuel cells (DMFCs) are one of the most efficient power sources that have the potential to be used in portable electronics applications, co-generation systems, and the automobile industry. They have unique advantages such as the ability to directly convert chemical energy into electrical energy with efficiency up to 70%, and they produce less polluting emissions. It is widely accepted that the catalytic performance of metal catalysts depends not only on their

geometry and dimension, but also on their support as well. Therefore, Pt and Pt alloys are applied as catalysts in DMFCs for methanol electro oxidation in acidic solutions [3].

Researchers believe that the electrochemical reaction mechanism of methanol takes place in dual pathways both directly and indirectly. The direct path is via weakly adsorbed intermediates. Likely candidates for such intermediates are formaldehyde and formic acid. The indirect path, which is more accepted, involves a strongly adsorbed intermediate, which is commonly accepted to be CO [4]. While Pt is the most active anode catalyst, cost and durability issues still hinder large-scale commercialization. Therefore, to overcome these obstacles, various binary and cluster Pt-based catalysts have been developed, such as Pt-SnO$_2$/CNTs (carbon nanotubes) as reported [5]. Such metal oxides are WO$_3$, CeO$_2$, MnOx, and RuO$_2$ all show enhancing in catalytic activity for methanol electro-oxidation [6].

Moreover, it was suggested that Pt-SnO$_2$/CN (Nitrogen doped carbon) had a high performance in methanol oxidation process [7]. Well dispersed Pt-SnO$_x$ nanoparticles supported on multiwall CNTs were reported by Hu *et al*., effectively averting CO poisoning and leading to improved efficiency [8]. Therefore, exploring new catalysts, improving catalyst activity and stability, durability, and reducing catalyst cost are currently the major tasks in fuel cell technology and commercialization.

Recently, Sasaki and co-workers summarized that Pt as a metal could be oxidized at a high potential, causing a decrease in active sites on the surface layer of the Pt [9]. Fuel cell performances are highly dependent on the oxidation states of the Pt crystallites on the surface of the catalysts. It was proposed that some non-noble metal oxide could prevent CO poisoning [10]. Generally, the effect of the promoters on the electro-catalytic activity

of platinum nanoparticles can be explained based on two major phenomena: the bifunctional mechanism and the ligand effect [11]. Because of the extraordinary thermal, mechanical and electrical properties, CNTs were used as a support for the catalyst [12]. However, the pristine surface of carbon materials is inert, making it a difficult substrate to attach metal catalyst particles. Therefore, it is of vital importance to develop effective techniques to improve adhesion through surface modification of carbon materials before metal deposition such as Pt can be attached directly onto such surface [13].

Generally, CNTs are surface functionalized before Pt attachment. In our work, tin oxides SnO_2 with titanium dioxide TiO_2 have been investigated as a double metal oxides support for platinum. By this process, the thin coated layer of TiO_2 could be formed in the presence of –OH and -COOH groups. In this study, tin oxide SnO_2 is incorporated on doped TiO_2 coated on CNTs as a bifunctional element for the noble metal in catalytic oxidation of methanol at low temperature. The support was prepared via hydrolysis of tin di-hydrochloride ($SnCl_2 \cdot 2H_2O$) in hot water in the presence of coated CNTs. Then, Pt/SnO_2-C-TiO_2/CNTs (later abbreviated to PtSTC in chapters 2&3) were prepared by a straightforward in situ liquid phase reduction of K_2PtCl_4 as a metal precursor. The effect of TiO_2 with SnO_2 was very clear in terms of activity and durability. X-ray photoelectron spectroscopy (XPS) analysis indicated a high binding energy of Pt with both oxides. This observation combined with the result of the cyclic voltammetry of the catalysts in sulfuric acid revealed that there was no surface onset peak at high potential, indicating high electronic stability of Pt in the acidic medium [14].

1.1 General concept of fuel cells

Fuel cells are devices that generate power as electricity by a chemical reaction. As shown in Figure 1, every fuel cell has two sided electrodes, one positive and one negative, called, respectively, the anode and cathode. In addition, the fuel cell has a membrane that transports the positive ions from anode to cathode. The reactions that produce electricity take place at the electrodes. On the anode, the oxidation reaction takes place generating electrons to the external circuit as a current and positive ion that pass through the membrane to meet the anions that are produced on the cathode,
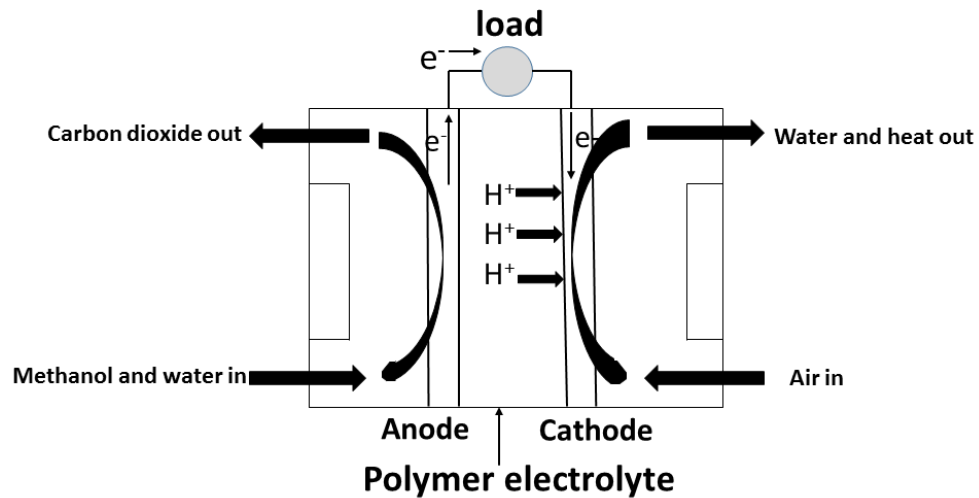
Figure 11.Basic features and operating principles of methanol fuel cell.

where the reduction reaction takes place. Every fuel cell also has a unique electrolyte which carries electrically charged particles from one electrode to the other, and a catalyst which speeds the reactions at the electrodes. There are different fuel cell feed types such as hydrogen, methanol and ethanol fuel cells. Each feed has its own operating conditions and different catalysts that could be used to produce the electric.

1.2 Types of fuel cells

There are several kinds of fuel cells, systemized mainly by two groups depending on the operation conditions like the temperature and the electrolyte type. Table 1 below lists the major types of fuel cells.

Table 1. Different types of fuel cells, main properties and operating conditions.

Fuel cell type	Operating Temperature (C)	Electrolyte	Fuel	oxidant
Polymer electrolyte membrane fuel cell	70- 120	Ion- exchange membrane	H_2	O_2, air
Direct methanol fuel cell (DMFC)	70-90	Ion- exchange membrane	methanol	O_2, air
Phosphoric acid fuel cell (PAFC)	180-220	Phosphoric acid	Natural gas Gasoline disesel	O_2, air
Molten carbonate fuel cell (MCFC)	650-700	Molten alkali carbonate	Carbon gas, bio gas, natural gas	O_2, air,CO_2
Solid oxide fuel cell (SOFC)	800-1000	Yttria- stabilized zirconia	Carbon gas, bio gas, natural gas	O_2, air
Alkaline fuel cell (AFC)	60-90	Aqueous alkline solution	Pure H_2	Pure O_2

1.3 Reactions of fuel cells

1.3.1 Hydrogen fuel cell

In the H_2 fuel cell, hydrogen is oxidized electrochemically at the anode electrode where the electrons are produced. On the other hand, oxygen is reduced electrochemically at the cathode as shown in Figure 2. Hydrogen fuel cells work relatively at low temperature (70-90 °C) [15].
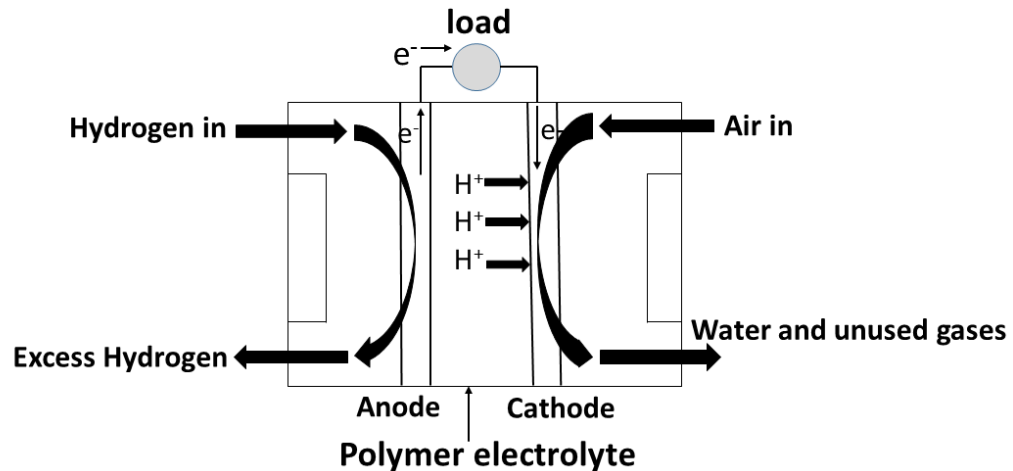
Figure 2 Basic principles of Hydrogen fuel cell.

Hydrogen is continuously supplied from a compressed storage tank to keep the electron flow. Oxygen is usually taken from the air and goes to the cathode. On both of the anode and the cathode, there is a functional catalyst. At the anode, the catalyst adsorbs the hydrogen afterward the oxidation reaction occurs, and it takes a few steps to complete the reaction. On the cathode, oxygen is adsorbed on the catalyst surface and is reduced to an anion that could meet the incoming positive (H^+) from the anode side and produce the H_2O as shown below in the reaction steps:

Anode Reaction: $\qquad H_2 \rightarrow 2H^+ + 2e^-$ $\qquad\qquad\qquad$ (1)

Cathode Reaction: $\qquad 0.5O_2 + 2H^+ + 2e^- \rightarrow H_2O$ $\qquad\qquad$ (2)

Overall Cell Reaction: $\qquad H_2 + 0.5O_2 \rightarrow H_2O$ $\qquad\qquad$ (3)

Hydrogen fuel cells face challenges in the operating condition and the feed purity. First, the high storage tank pressure could make a deadly explosion. Second, the feed purity is still a complicated obstacle. Since the hydrogen is produced from the fossil oil sources, the carbon monoxide content is a destructive material that poisons the catalyst active sites. Thus, the trace of CO must be converted to CO_2 by a catalytic process to reduce the CO to <10 ppm before the fuel gas enters [16].

1.3.2 DMFCs

DMFCs are devices that transform the chemical energy of methanol to electrical energy directly, with high efficiency up to 80-85%. Methanol is electrochemically oxidized at the anode, whereas the oxidant, the oxygen, comes from the air which is reduced at the cathode. Generally, methanol is the smallest alcohol molecule and is the most studied one. Small organic molecules containing one or two carbon atoms are one of the tricky catalytic issues. The oxidation of methanol involves six electrons which make the mechanism quite complicated. In 1988, Parson and Van der Noot presented their theory about the alcohol electrochemical oxidation reaction. They assumed that the methanol will undergo dual pathways which consist of two routes to get the complete reaction done as shown in Fig. 3 [17].

One is called the indirect pathway involving a strongly adsorbed intermediate. This intermediate is commonly accepted to be CO. The main obstacle of this pathway is how to oxidize the carbon monoxide. Another pathway is the direct path involving weakly adsorbed species which could be formaldehyde and formic acid. Besides that, in 1975, M. Watanabe, S. Motoo stated the presence of another element with platinum can enhance the activity of the catalyst according to the bifunctional theory. The theory states that the

platinum will adsorb the methanol leading to one of the pathways explained above. On the

other hand, the bimetal will activate the water that could react with the carbon monoxide

forming CO_2.
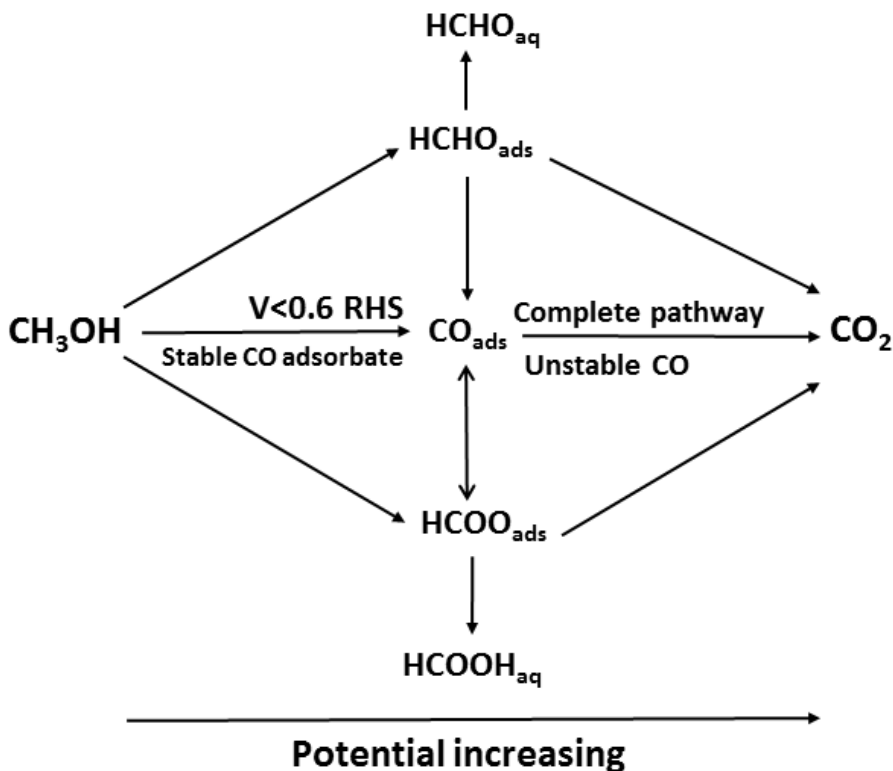
Figure 3. Shows the dual pathway mechanism [17].

1.4 Catalyst literature review

Heterogeneous catalysts are the most successful substances found to decrease the

severe reaction conditions. The catalysts have seen many improvements for the last few

decades. Such advances are modifying the parent metal to alloys or metal oxides

incorporated to be bi-metallic or bi-oxides catalyst supported. The bi-oxides technique has

emerged to be the most interesting technology that provides high stability and activity regarding fuel cell applications [18]. So, understanding and finding the hidden properties of bi-oxides supported catalysts have become a necessity. Also, their surfaces show unique properties that do not exist in the monometallic catalyst surface [19]. Nevertheless, knowing how the chemical and electronic properties could be altered according to the original metal still faces some challenges. Many investigations have been devoted to studying the binary oxides or mono-oxide supported catalyst surfaces [20]. Park *et al.*, have stated two reasons that contribute the modification of chemical and electronic properties. First, the strong interaction between the noble metal and the metal oxide alters the electronic configuration of the surface, which is called the ligand effect. Second, metal oxides have a high amount of hydroxyl groups which could serve as co-catalysts of noble metal, based on bifunctional mechanism [21].

In our current work, a noble metal (Pt) supported on a non-noble metal oxide catalyst has been chosen for two reasons. First, they have wide applications in different areas because of their abundant sources, low cost, and environmental acceptance. Second, they have distinguished corrosion resistance in the electrochemical environment of PEFCs compared with carbon material supports because the noble metals in oxides exist in high binding energy and do not readily lose further electrons to be further oxidized. Thus, to date, they are the most common group used on electro-catalytic applications. However, other non-platinum bi-metallic catalysts exhibit interesting outcomes and important applications as well. For instance, the Au-Ag catalyst is used for carbon monoxide oxidation due to the strong synergistic forces between the two metals [22]. However, using noble metals costs a lot of money which is not practical if it is used on a commercial scale.

Another aspect regarding the high activity and durability is the catalyst support. In this review, we are trying to demonstrate and cover the mostly used catalyst supports. We will also focus on an important utilization of the catalysts in alcohol oxidation reaction such as methanol.

1.4.1 Catalyst Support

PEM fuel cells are still not practical for market needs and are inhibited in broad applications due to two great challenges; the high cost production catalyst and poor durability and reliability [23]. Therefore, using a proper catalyst support is highly recommended; using supported catalysts shows a great influence regarding the cost and durability [24]. Most of the currently Pt-based catalysts are supported on porous and conductive carbon with a high specific area. The support material is essential to obtain a high dispersion and uniform distribution which lead to enhancing the catalyst performance. Moreover, some of the supports play a role as co-catalyst that reinforces the catalyst. Such supports are transition metal oxides like TiO_2 [25], ZrO_2, and WO_2 [26]. They support not only the activity enhanced by the oxide support incorporation but also the durability. In summary, the catalyst supports to be considered as a commercialized product should meet the following conditions: 1) high specific area in which the catalyst could be dispersed, 2) high electrochemical stability, 3) conductive, and 4) the interaction between the metal and the support should be accounted to improve the catalyst durability [27]. Regarding carbon based supports, there are three carbon-based popular catalyst supports: carbon black, CNTs, and graphene. Vulcan XC-72 carbon black is considered the most popular supporting material. In addition to the recently increased uses, much work has been done to developing novel catalyst supports, including nanostructured carbons such as CNTs, carbon nanofibers

(CNFs), and metal oxides. Oxide coated CNTs can also be activated by other conductive atoms such niobium, or compounds to enhance both the catalytic activity and durability of the resultant catalysts. In the next part, we report the three kinds of carbon-based supports. We also demonstrate their activities in the methanol oxidation reactions with and without metal oxides in co-existence. We will point out the crucial presence of a metal oxide on carbon material substrates and how to enhance the kinetics, durability, and stability.

1.4.1.1 Pt-based supported with and without metal oxides on carbon in DMFCs

Vulcan XC-72 carbon black is considered the most popular supporting material. However, there are more than one types of carbon material such as mesoporous carbon, activated carbon and XC-72 carbon black. Each one of them has a unique morphology, activity and surface area [28]. For instance, mesoporous carbon has pore sizes in the range 2-50 nm which can be classified into two types: the ordered mesoporous carbon (OMC) and disordered mesoporous carbon (DOMC). The proper pore size is crucial. For instance, the DOMC exhibits large pore size which could lower the conductivity and makes any metal deposited irregularly distributed, leading to diminished catalyst performance. On the other hand, a study was conducted by using OMC as a catalyst support, and the results were reported by comparing Pt/C and Pt/GMC at the same metal loading 20% [29]. The authors reported enhancing the current density from 27.1 mA/cm^2 in Pt/C to 37.5 mA/cm^2 in Pt/GMC. In contrast to Vulcan XC-72, the mesoporous carbon shows distinguished properties such as surface area and three dimensional interconnected mesoporous net. Subsequently, extensive studies have been devoted to using mesoporous carbon in fuel cells [30]. Yu *et al*., investigated the effect of the pore size in range [10-100 nm] in catalytic activity of the supported PtRu in DMFCs [31]. They found at 25 nm pore size, the activity

11

was the higher by a 43% increase comparing to commercially catalyst [32]. Then, they stated that not only the pore size or the pore volume is the reason of the activity, but it is also highly interconnected pore system that permits an effective mass transport [33]. For that finding, a mesostructured composite catalyst Pt-SnO$_2$/GMC was investigated in methanol electro-oxidation [34]. They compared the activity with the commercial catalyst Pt/C. They found after oxide incorporation there was an increase in catalyst activity (Figure 4A) and negative shift in oxidation peak as in Table 2. Also, they attributed that to two aspects: first, the unique pore size of the support and 3D pore channel provided 4 nm room for Pt nanoparticles to disperse and made it accessible for methanol to diffuse. Second, the SnO$_2$ presence, which could assist the Pt in methanol oxidation, could activate the water at a low potential. In addition, we can see in Figure 4B that the 20PtSnO$_2$/GMC has a high durability after 600 seconds.

Table 2 Electro-catalytic activity parameters of the catalysts for methanol oxidation. Ref. [34].

Catalyst	Maximum current density/mA cm^{-2}	Maximum current density/mA mg-Pt^{-1}	Potential of maximum current /V
20Pt/GMC	34	481	0.75
20PtSnO$_2$/GMC	45	1273	0.68
20 wt.%Pt/C	26	368	0.70
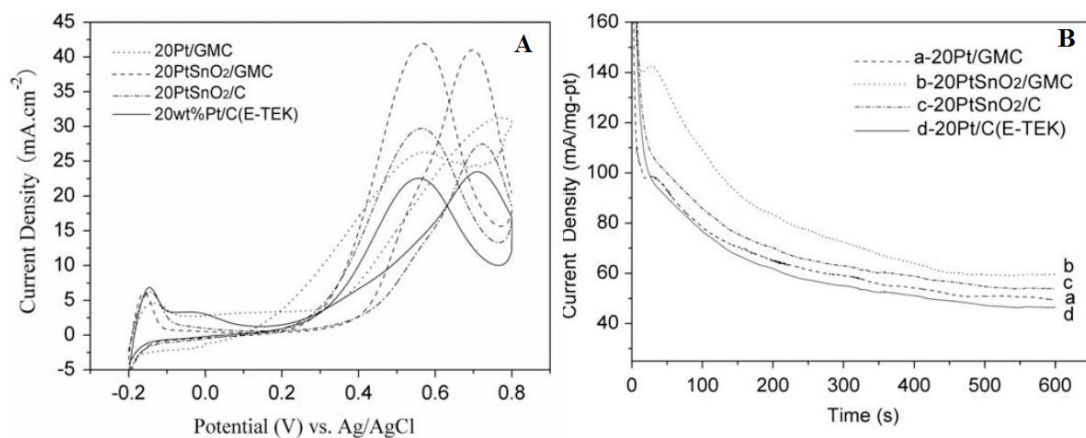
Figure 4. A) Cyclic voltammetry curves of catalysts toward methanol oxidation in 0.5 MH2SO4 + 0.5 M CH3OH solution with a scan rate of 0.05 V.s^{-1} at 298 K, (forward scan: 0.2 – 0.8 V and reverse scan: 0.8 – _0.2 V), B) Chronoamperometry curves of samples for methanol oxidation at 0.55 V,298 K. Ref. [34].

Carbon black under DMFC operation conditions suffers from two constraints: carbon corrosion at high potential leading to loss in the catalyst surface area and reducing the catalyst durability [35]. A study was conducted by utilizing carbon black to determine its resistance under fuel cell operation conditions, and they compared it with carbon nanostructure [36]. They found a reduction in surface area 35% in Pt/CB and 20% in Pt/CNP after 15 hr. Also, they reported surface area loss rate 0.0032 m^2/g.hr^{-1} and 0.00152 m^2/g.hr^{-1} for Pt/C and Pt/CNs, respectively. Consequently, many researchers have started modifying carbon black surface with other materials, or replacing it with metal oxides [37]. A study functionalized the CB with silicon oxide and tin dioxide to overcome on the Pt aggregation [38]. They used SnO_2 as a catalyst promoter and SiO_2 as a stabilizer; in addition, they reported increasing in the oxidation state of the platinum by 0.6 eV. They found that at 0.9 V the Pt/C-Sn$_{0.3}$Si$_{0.7}$O$_x$ the current is about 1.5 times in Pt/C. They concluded that the coexistence of incorporated binary oxide prevented the carbon corrosion to Pt and protected the SnO_2 from dissolution.

1.4.1.2 Pt-based supported with and without metal oxides on graphene in DMFCs

The second popular carbon material support is the graphene. In 2004, graphene was first discovered experimentally by Giem and his co-worker at Manchester University by a peel-off technique [39]. Technically, there are more than one allotrope of the graphene which are one dimensional and two dimensional; however, the latter was thought to be not stable thermodynamically at certain temperatures [40]. Graphene has distinguished properties such as high surface area (2600 m^2/g), good electrical conductivity, chemical stability and intrinsic mobility (15000 cm^2/vs) [41]. These unique properties made graphene a proper candidate for many applications. For instance, it could be applied as a transparent electrode in solar cells and light emitting [42]. Considering the fuel cells, there is a rapidly growing interest in utilizing the graphene in the electrochemical application such a catalyst support. Another form of graphene is graphene oxide which is manufactured by breaking the graphite sheets apart by acid oxidation and physical agitating like sonication [43].

Therefore, many researchers have devoted their intensive work to use graphene in fuel cells [44]. Comparing to CNTs, graphene has a much higher surface area and conductivity; however, graphene production cost is much higher than CNTs and the carbon black. Since the fuel cells are considered as an upcoming alternative power source, great work must be done to reduce the cost and enhance the efficiency. Thus, using the strong catalyst support such as graphene could achieve the target in term of the efficiency. Currently, the most fuel cell issues are overpotential in cathode side, poisoning intermediates species such as carbon monoxide in anode side, and fuel crossover in the interfacial membrane. [45]. Twenty percent of Pt/graphene has been used to increase ORR activity as reported by Balbuena,

Perla B *et al.* [46]. They stated that the deposited Pt particles decorated the graphene surface with small sizes which attributed to a high surface area. Also, they reported enhancing in methanol oxidation performance. Another study by Liu and co-workers functionalized the graphene surface sheets (FGS) by the thermal expansion of graphene oxide [47]. They found the Pt/FGS exhibits high current density and good retention on the electrochemical surface area after 5000 cycles. Further investigation has been devoted to Pt/RGO composites which were prepared in situ chemical reduction of graphene oxide and H_2PtCl_6 using $NaBH_4$ as a reducing agent [48]. Compared to commercial Pt/C, the ECSA, current activity and peak positions were found the best in Pt/RGO. A fast kinetic reaction was found in Pt/RGO, which shows that the onset potential shifted to a more negative potential as shown in Figure 5.
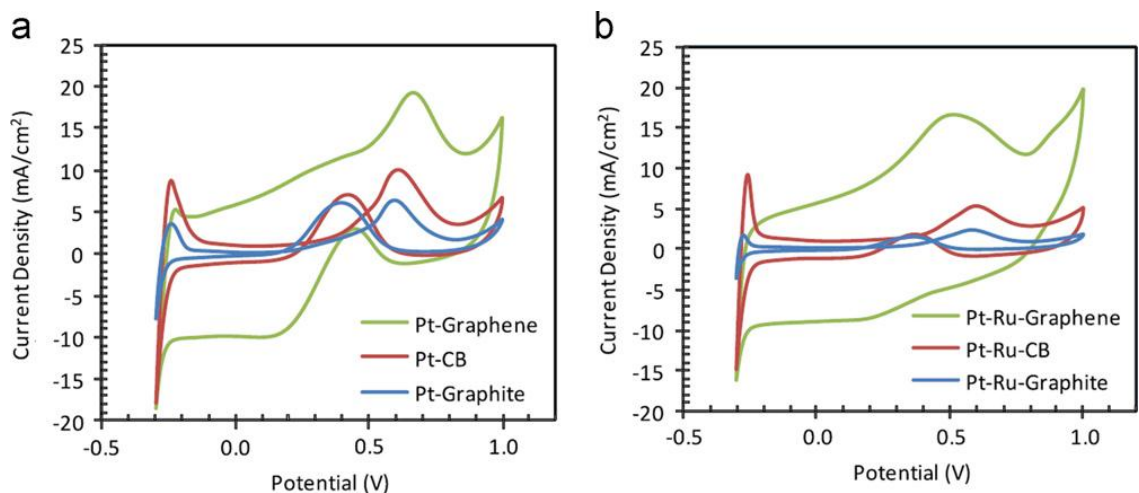
Figure 55. Cyclic voltammograms of (a) Pt nanoparticles and (b)Pt–Ru nanoparticles on different carbon-based supports in1M CH_3OH/0.5MH_2SO_4 at 50mV/s. Ref. [48].

The high performance of Pt/graphene could be attributed to the robust interaction between Pt particles and graphene Nano-sheets [49]. Considering the methanol oxidation reaction, there are several parameters that assess the catalyst performance. First, the forward and backward peak ratio can refer to the catalyst CO-tolerance indicator. Second,

onset starting reveals the pace of the catalyst reaction kinetics to reach a current peak early. Pt/graphene shows good I_f/I_b ratio as depicted in Figure 5 for methanol oxidation which refers to complete reaction path with less carbonaceous species residue such as CO [50]. Owing to the bi-function theory, Ru decorated with Pt could promote the methanol oxidation to occur at a more negative potential. It was suggested that the Ru will activate the water (O-H-O) at a low potential, reacting with Pt-CO adsorbate. Wang and co-workers elucidated the synthesis of Pt on Pd- nanoparticles as a bi-metal on graphene via a wet chemical approach as shown in Figure 6 [51].
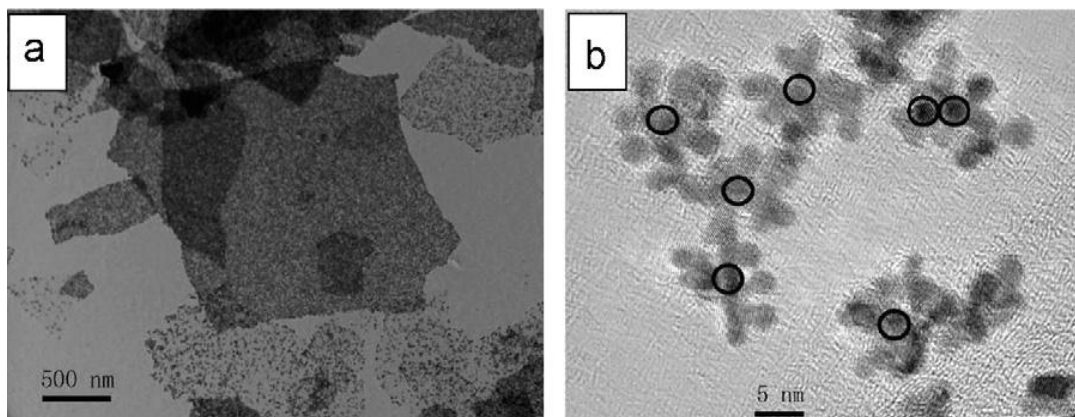
Figure 6. TEM (a) and HR-TEM (b) images of TP-BNGN. The circled parts in panel B denotes as Pd nanoparticles. Ref. [51].

Pt particles formed on Pd-core graphene nano-sheets. The prepared catalyst shows high electrochemical surface area 81.6 m/g and 54.7 m/g for Pt-Pd/graphene and Pt/C, respectively. However, keeping the expensive metals as a helper catalyst is not affordable. Recently, a study investigated a novel nanostructured support of ZrO_2/nitrogen-doped graphene Nano sheets (ZrO_2/NGNs) as a support for Pt in methanol oxidation [52]. They used the atomic layer deposition (ALD) method to deposit the ZrO_2 on NGNs, which is as they reported the ALD technology can control the oxide size and the distribution of metal oxides. They reported results as shown in Figure 7a. An enhancement in the catalyst

activity and the surface area after oxide incorporation as in Pt-ZrO$_2$/NGNs was 2.1 times

higher than that in Pt/NGNs with 65 m^2/g and 48 m^2/g, respectively. Also, they found a

high catalyst stability and durability after 4000 cycles in the Pt-ZrO$_2$/NGNs surface which

was 50.2% of the initial; however, in Pt/ NGNs it was 23.5%.
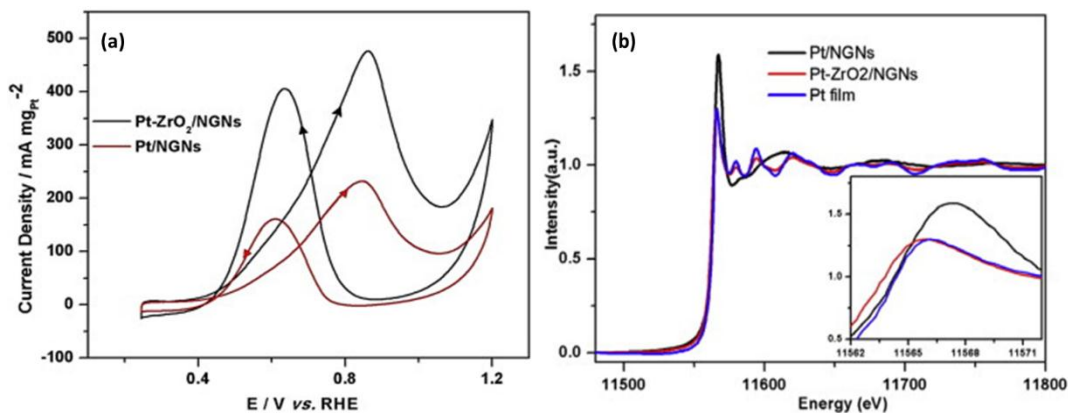
Figure 7. (a) Cyclic voltammograms of Pt/ZrO$_2$/NGNs and Pt/ NGNs electrodes in 1 M CH$_3$OH +0.5 M H$_2$SO$_4$ solution at scan rate of 50 mV s^{-1}. (b) XANES spectra of Pt L3 edge of composite electro-catalysts. Ref. [52].

Consequently, they decided to study the triple the interaction in ZrO$_2$-Pt-NGNs by

using XANES spectra of PtL3. They found an absorption energy 11567 eV which refers to

2P$_{3/2}$ to 5d transition. The Pt-ZrO$_2$/NGNs has lower intensity than Pt/NGNs. As shown in

Figure 7b, they interpreted the last observation to the less electron vacancies in 5d orbital,

which is reasonable evidence of the electron transfer resulting from the stronger metal

support between Pt and ZrO$_2$/NGNs [53]. Concluding from the last study mentioned, the

presence of a metal oxide as a Pt co-support enhanced the noble metal stability and activity

even in using the graphene as a support. In the next part, we will illustrate the use of CNTs

as a catalyst support, which is the related work of this thesis.

1.4.1.3 Pt-based supported with and without metal oxides on carbon nanotubes
 in DMFCs

In 1991, Iijima discovered the CNTs during the fabrication of fullerene by arc discharge [54]. Due to the fascinating properties of CNTs, carbon nanotubes are applied in many usages such as gas storage material, energy storage material, electronics and catalysis [55]. In our current review, we present the application of the CNTs in electro-catalysts as a support. Because of the chemical stability and electronic conductivity, CNTs have been chosen by many researchers to utilize them in fuel cell catalysts and photo catalysis. However, the pristine surface of the CNTs is chemically inert. Thus, they need to be functionalized by either chemical agents or electrochemical techniques. Once they are modified, the CNTs possess different types of oxygen species such as hydroxyls, epoxies, and carboxylic groups [56]. Surface functionalization can increase the hydrophilicity or the wettability of the CNTs in water. The oxygen-containing groups can serve as active hosts for subsequent by covalent, electrostatic and hydrogen bonds. Additionally, a proper amount of oxygen-containing species on the CNTs could lower the activation energy and facilities electronic transfer. Nevertheless, extreme oxidation could disrupt the CNTs backbone or make severe corrosion [57]. To address this issue, ionic liquid polymer (PIL) was used as an agent to introduce a large number of oxygen groups on the CNTs surface as reported by Wu *et al*., [58]. On the same a nonacid treatment track, Wang *et al*., used 1-aminopyrene to modify the surface [59]. Different oxidants and different oxidation conditions introduce various kinds of oxygen groups. For instance, air oxidation generates more phenol [60]. However, using nitric acid which is the most used oxidant for carbon surfaces gives more -C=O groups, whether the nitric acid was diluted or concentrated [61]. According to the outstanding reported properties for CNTs, the CNTs by themselves could

be used as a non-metal catalyst such as in a nitrobenzene hydrogenation reaction [62]. The CNTs as a catalyst support has advantages such as less inner diffusion of reactants and products, π- interaction between Pt and CNTs [63]. Moreover, there is a high mass transfer through the 3D network and electronic conductivity and good metal dispersion. In addition to that, the sp-c vacancies on the CNTs surface could enhance hydrogen adsorption which is an indicator of affinity to C1-3 alcohols [64]. Unlike other carbon materials catalyst supports, CNTs exhibit remarkable result regarding hydrogen fuel production by using microwave assisted dehydrogenation [65]. Also, CNTs show much higher resistance against poisoning than carbon black XC-72 [66]. Owing to the mentioned CNTs advantages, many people have begun decorating various metals on the CNTs surface. A study reported 20% Pt/MWCNTs activity in DMFCs and compared that with Pt/C XC-72 [67]. The authors stated that the current density was 14.7 mA/mg Pt and 3 mA/ mg $_{Pt}$ for Pt/MWCNTs and Pt/C XC-72, respectively.

A major breakthrough is reported to deposit the Pt-Ru on CNTs as reported by He *et al*., [68]. The prepared catalyst Pt-Ru/CNT showed remarkable forward peak to backward ratio and enhanced kinetics. In addition, they investigated the Pt/Ru ratio on the forward peak potential position. As shown in Figure 8a, the authors have stated that at low platinum loading the methanol reaction shifts to a more negative potential. This is because of the Ru ability to adsorb and activate the water at a low potential [69]. Nevertheless, reducing Pt loading with increasing Ru content ratio could retard the catalyst activity since Ru has no catalytic activity toward the electro-oxidation of methanol as Figure 8b depicts [70]. Also, Ru is still expensive which is the major impractical issue.
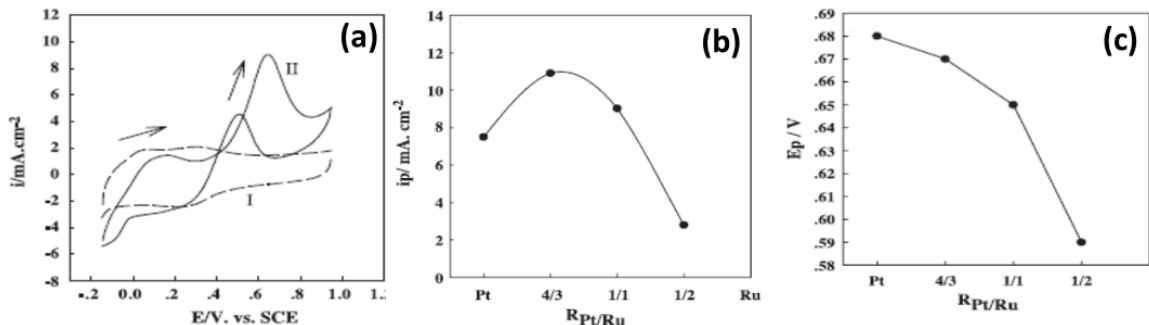
Figure 8. (a) activity of PtRu/CNTs in Methanol (b) shows Pt/Ru ration effect on peak Potential position, (c) show catalyst activity with Pt/Ru ratio, (a) activity of PtRu/CNTs in Methanol. Ref. [70]

Investigators have made considerable efforts to avert catalyst poisoning by CO-like intermediates. Alloying Pt with Ir, Ni, Co, Ru and Sn as metals or their oxides has become the most interesting topic for the researchers. PtRu has shown a superior performance regarding complete CO_2 production; however, Ru still is expensive which makes the catalyst non-feasible. To make the catalyst commercially practical, it was recommended that decorating a non-noble metal oxide could enhance the Pt activity, durability, and at less cost [71]. In the direct methanol fuel cells, methanol oxidation mechanism has sequential steps. The first step is methanol adsorption on the catalyst. Next, dehydrogenation will take place. Then, the formate species or the carbon monoxide will form. The faster kinetics is, the more functional catalyst is needed, and that has been achieved by adding the second element with Pt. The indicator is called the "onset potential position." The earlier peak onset marks how fast the kinetic is. Incorporating the metal oxide could affect it in two ways: either altering the Pt electronic structure called the "ligand effect" or adsorbing and activating the water at a low potential which is called the "bi-function technique". Coupling both is also possible; however, it was stated by Lu *et al.*, [72] based on UHV, NMR and electrochemical studies that bi-functional rout influence

20

is higher than ligand by four times. Chuangang *et al*. reported that Pt-SnO$_2$/HQ-MWCNTs showed distinguished results in methanol oxidation reaction [73].
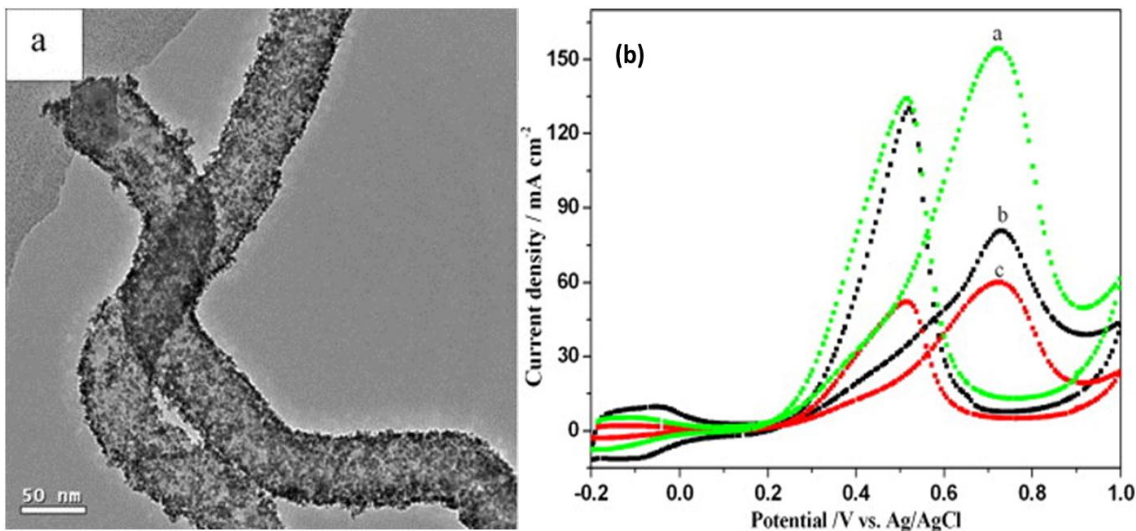
Figure 9. (a) TEM of Pt-SnOx/HQ-MWCNTs catalyst (b) Cyclic voltammograms of: (a) Pt-SnOx/HQ-MWCNTs catalyst, (b) JM 20% Pt/C catalyst, and (c) Pt-SnOx/AO-MWCNTs catalyst in 0.5M H2SO4 and 0.5M CH3OH solution saturated by N2 with the scan rate of 50mV.s^{-1} at 20±1 ∘C. Ref. [73].

Such results were early onset at 0.18 V at Ag/AgCl and there was a high forward current density peak up to 150 mA/cm^2 at 0.74 V vs. Ag/AgCl. They stated also well-dispersed of Pt-SnO$_2$ and covered most of 8-hydroxyquinoline HQ-MWCNTs. In addition, they described the catalyst tolerance toward incomplete carbonaceous species by calculating the forward to backward peak ratio. The early peak observation could be assigned to the SnO$_2$ presence in the Pt vicinity with high Pt 4f binding energy (71.9eV) that enhances the CO-removal mechanism since the Pt has less affinity to bond with CO adsorbate. Another study demonstrated reducing Pt loading to 10% with titania rutile phase with Nb as a dopant NTO/CNTs and compared it with Pt/CNTs at the same loading [74]. They found a modest difference in surface area of 36.8 m^2/g and 21.4 m^2/g for Pt/NTO/CNTs and Pt/CNTs, respectively. In addition, increasing in the binding energy 71.2 eV to 71.5 eV was noticed

21

which is attributed to a strong interaction between Pt particles and the NTO/CNTs support. In Figure 10a, methanol oxidation onset was noted early at 0.2 V (vs. Ag/AgCl) and 0.275 V (vs. Ag/AgCl) for Pt/NTO/CNTs and Pt/CNTs, respectively.
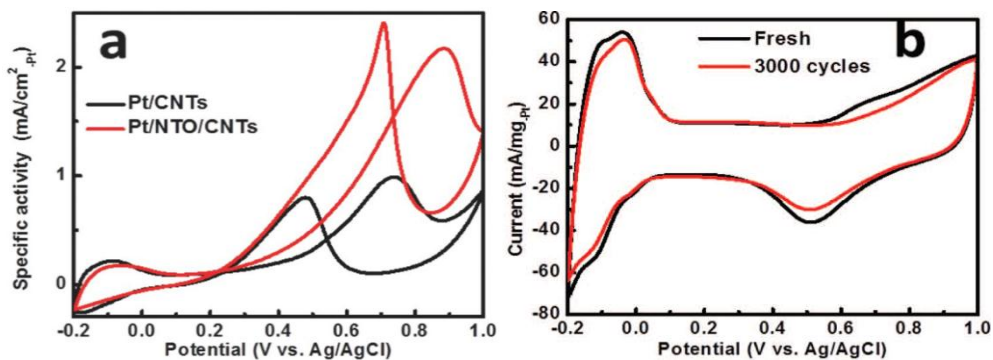
Figure 10. (a) Specific activities of methanol oxidation on the Pt/NTO/CNTs and Pt/CNTs catalysts in N2-saturated 0.1 M HClO4 solution with 1.0 Methanol, (b) CV of initial cycleand that after 3000 cycles for Pt/NTO/CNTs with scanning rate at 50 mV/s. Ref. [74].

However, they reported electrochemical surface area (ECSA) loss after 3000 cycles in Pt/NTO/CNTs less than in Pt/CNTs as in Figure 9b. In this sense, we could infer that even in CNTs the Pt could be corroded, or even aggregated. Platinum deposited on ZrO_2/CNTs and ZrO_2/C was examined in DMFCs [75]. The study reported a surface area 211.59 m^2/g, 69.60 m^2/g for Pt/ZrO_2/CNTs and Pt/ZrO_2/C, respectively. Also, they found a more negative methanol onset potential in Pt/ZrO_2/C of about 0.587 V, and in the case of Pt/ZrO_2/CNTs the onset was 0.208 V (vs. Ag/AgCl). However, Pt/ZrO_2/CNTs showed high I_f/I_b about 2.2; nevertheless, Pt/ZrO_2/C exhibited 1.61. Another study incorporated Pt onto Ru-doped SnO_2 [76]. The study reported 0.23 V vs. Ag/AgCl onset potential with high forward to backward ratio. They attributed the good performance to: first, reducing the CO-poisoning effect. Also, there was Ru existence with tin dioxide that generates more hydroxyl groups at low potential from water dissolution. Moreover, Ru improved the SnO_2 conductivity which enhanced the methanol electro-oxidation. Dou *et al*, have utilized SnO_2

as a durable catalyst support avoiding the carbon corrosion at high potentials [77]. They found remarkable Pt stability at high voltage and less ECSA loss in Pt/SnO_2 11.3% compared to Pt/C 64.7%. Even though they showed good stability, no solid explanation was presented. They attributed that to the strong Pt and SnO_2 interaction which was consistent with the Pt 4f XPS result. Nevertheless, their statement regarding no electron supply is theoretically unconvincing. Another study was made by pulse electrodeposition of Pt on porous TiO_2 thin film. They improved the electric conductivity of TiO_2 by thermal annealing in a vacuum 0.1 Torr. They stated a high surface area 172.9 m^2/g and good forward-backward current ratio 1.44. In addition, they mentioned 0.327 V (vs. Ag/AgCl) as an onset potential [78]. Another study was done by preparing a composite by deposition of PtRu hydrothermally on $SnO_2/CNTs$ [79]. They claimed a difficulty with SnO_2 deposition on the CNTs, so they utilized ethylene glycol and polyvinyl pyrrolidone (PVP) to assist tin oxide deposition. They found a high surface area, current density and appreciable Pt stability at a high potential. Additionally, they attributed that to homogeneous and porous SnO_2 layer over CNTs. In addition, $Ru-SnO_2/CNTs$ modified the electronic properties of Pt; moreover, hydrothermal synthesis supplied a uniform environment for nucleation and growth of metal particles. However, they reported a high onset potential around 0.37V (vs. Ag/AgCl). Song *et al*., investigated $TiO_2-Pt/CNTs$ after heat treatment at 200 °C for 2 hrs. They found that there was no effect on the Pt crystal phase after heating in the presence of the titanium dioxide, which remained in hydrous form. Also, they stated that the Ti-OH hydrous form could accelerate the CO adsorbate oxidation reaction rather than need to activate the water from the electrolyte. They reported

1.11 mA/cm^2 as the forward current activity and surface area 51.5 m^2/g; however, the onset was 0.407 V (vs. Ag/AgCl) [80].

In our present work, we uitilized two metal oxides, titanium dioxide as a coating agent to coat the CNTs and tin oxide as a Pt reinforcer agent and denoted as Pt-SnO$_2$-C-TiO$_2$/CNTs. According to the Pt 4f XPS spectra, the binding energy shifted to the high oxidation state of the platinum. A high oxidation state means high electrons back donation from Pt to both oxide which renders the Pt to oxidize the carbon- adsorbates at low potential. We observed the lowest methanol onset potential (0.11 V. vs Ag/AgCl) and methanol oxidation peak potential (0.62 V. vs Ag/AgCl). In addition, we recorded a high catalyst activity in PtSTC (2.4 mA/cm^2) compared with (1.98 mA/cm^2) in PtSC and (0.98 mA/cm^2) in Pt/C. Thus, the binary metal oxides idea could be considered a succsseful method for methanol oxidation.

In summary, regarding carbon material supports, each catalyst support serves uniquely and shows a different performance in different applications. Carbon black is the cheapest carbon material that is used as a catalyst support. It has good performance in an oxygen reduction reaction since it provides four electrons which yield water as a final product. Compared to the CNTs and carbon black, graphene has more surface area and high intrinsic mobility. However, the production cost of graphene is higher than both CNTs and carbon black. Conversely, CNTs have a strong penchant to adsorb the hydrogen and small alcoholic organic molecules such methanol and ethanol. CNTs show much higher resistance against poisoning than carbon black XC-72. Also, CNTs exhibit outstanding results regarding hydrogen fuel production by using microwave assisted dehydrogenation. As a consequence, they are applied as a catalyst support in the direct methanol fuel cells.

Despite all the advantages reported above for carbon material as a support catalyst, it must be mentioned that they have insufficient corrosion resistance in in the overall long term operation. Thus, replacing carbon catalyst support by inorganic metal oxides is one of the solutions people have started trying to work on. On the other hand, some people have kept using CNTs, CB and graphene by coating or incorporating other metal oxides on their surface.

CHAPTER 2. Catalyst Preparation and Characterization Methods

2.1 Catalyst preparation

2.1.1 Carbon nanotube coating by titanium dioxide

Multiwall CNTs (purity >95%, diameter 35-60 nm) were obtained from NanoLab. $SnCl_2 \cdot 2H_2O$ was purchased from Acros Organic. Potassium tetrachloroplatinate (K_2PtCl_4) was supplied from Alfa Aesar. Titanium isopropoxide ($C_{12}H_{28}O_4Ti$, 99.9% metal basis) was purchased from Sigma Aldrich. A desired amount of CNTs was treated with 3:1 H_2SO_4–HNO_3 (volume ratio) in an ultrasonic bath at 60 °C for 2 hours for surface functionalization followed by filtration and a thorough washing with deionized water. In a sol-gel technique, 20 mg was treated and CNTs were dispersed in a solution containing 8 mL ethanol, 2 mL benzylalcohol plus excess water with aid of ultrasonication and stirring. A certain amount of titanium isopropoxide was dissolved in ethanol and slowly (drop-wise) dripped into CNT suspension with a pipette. After 2 hours of stirring, the final solution was vacuum-filtered, washed in ethanol, and dried at 80 °C in a vacuum oven overnight. The desired amount of TiO_2/CNTs was doped by carbon with 10% acetylene C_2H_2 in N_2 at 700 °C for 20 min at flow rate of 40 ml/s, which is denoted as C-TiO_2/CNTs.

2.1.2 Synthesis of oxides on CNTs

The coated and doped CNTs (15 mg) were dispersed in 8 ml of hot water at 70 ˚C and sonicated for 30 minutes followed by hydrolysis of 3.2 mg tin dehydrate chloride by stirring for 12 hours at 70 ˚C, to obtain 10% weight loading of the metal oxide. The above suspension was washed with deionized water during vacuum filtration and then dried in an oven at 70 ˚C for 8 hours. The black powder was then calcined at 600 ˚C under nitrogen gas for 1 hour. Pt/SnO_2-C-TiO_2/CNTs and Pt/SnO_2/CNTs catalysts were prepared by in situ liquid phase reduction

2.1.3. Preparation of Pt on metal oxide coated CNTs

Pt catalysts were prepared by a polyol process. The process was as follows: 10 mg of metal oxide coated CNTs were dispersed in the solution of 2.5 ml water and 2.5 ml ethylene glycol, followed by ultrasonication for 20 min. Then 1.87 ml (0.007M) of platinum

precursor was added (to achieve 20% loading), followed by 6 hours of stirring at 80 ˚C. After stirring, the obtained catalyst was washed with ample amount of deionized water to remove any ethylene glycol residue. Finally, the powder was placed in an oven at 70 ˚C for 8 hours. In this way, catalysts of $Pt/SnO_2/c\text{-}TiO_2/CNTs$ and $Pt/SnO_2/CNTs$ were prepared for study. These catalyst names, for convenience, were abbreviated to PtSTC and PtSC, respectively. Another catalyst prepared, $Pt/TiO_2/CNTs$, without carbon doping is abbreviated as PtTC.

2.2 Characterization and spectroscopic methods

2.2.1 Transmission electron microscopy

The transmission electron microscope (TEM, JEOL-1400-120kV) and FEI Tecnai F30 Twin -300kV) was used to determine the morphology of the coating layer on CNTs and to characterize size and shape of the Pt particles. A small amount was taken from the catalysts of PtSTC and PtSC and dispersed in ethanol under sonication. A drop of the prepared ink was transferred with a pipette and dripped on a TEM grid (400-mesh carbon-coated copper, Electron Microscopy Sciences). The specimen was left in the open atmosphere to dry rapidly. Then, the grid was examined by TEM and the results were taken to be analyzed.

2.2.2 X-Ray photoelectron spectroscopy

Oxidation states of the C 1s, Ti 2p, Sn 3d, O 1s and Pt 4f in the prepared catalysts were analyzed by X-ray photoelectron spectroscopy (XPS, Kratos Axis 165). The spectrometer is equipped with a concentric hemispherical analyzer which uses 8 channel Tron detectors. The sample was ion sputtered with a differential ion gun for 60 seconds at 4 kV. A Mg Ka anode, operated at 15kV and 225 W with a photon energy of 1253.6 eV, was used as the X-ray source. The base pressure of the chamber during inspection was 10^{-9} Torr. The pass energy was 80 eV during the survey scan and 20 eV for the windows scan [81].

2.2.3 X-Ray diffraction

X-ray diffraction (XRD, Philips X-pert) equipped with Cu Kα was performed to analyze the crystalline phase of the catalysts. The data were collected with a Philips X-pert diffractometer over an angle range of $2\theta = 20\text{-}90°$ at a scan rate of $0.026°$ s^{-1}. The results explained the crystalline structure of Pt and SnO_2.

2.3 Electrochemical methods

All electrochemical tests were carried out by an Electrochemical Workstation (BAS100) to study the electrochemical performance of the prepared catalysts and compare with a benchmark E-TEK catalyst Pt/C, all at the same Pt weight loading of 20%. An Ag/AgCl electrode and a Pt coil wire were used as the reference and counter electrodes, respectively, in a three electrode cell. The prepared catalysts were dispersed in ethanol and water to prepare an ink of 1 mg ml^{-1}. 10μL of the dispersed catalyst were dripped onto a polished carbon glassy electrode (5mm), followed by 5 μL of (0.05%) Nafion. Cyclic voltammetry (CV) was carried out at a scan rate of 30 mV s^{-1} in a 1.0 M H$_2$SO$_4$ electrolyte with nitrogen purge (for 15 min). The electrochemically active Pt surface area was determined by integration of the areas of the CVs in the potential region of under potential deposition of hydrogen, after double layer charge correction and taking into account the reference value of 210 μC cm^{-2} for full monolayer coverage. Measurements were carried out in 1.0 M H$_2$SO$_4$ + 1.0 M CH$_3$OH at a loading of 2:1 (20%:10%) to determine methanol oxidation reaction activity. To investigate the durability, *i-t* curves were obtained as well.

CHAPTER 3. Results and Methanol Electro-Oxidation Activity

3.1 Transmission electron microscopy results

Figure 11 (a) shows a TEM image of a thin layer of TiO_2 conformably coated on CNTs without aggregation. Low temperature carbon doping with slow heating during the doping process ensured that the coating would retain its shape without sintering. Figure 11 (b) illustrates the uniform distribution of tin oxide as well as Pt deposited onto the C-TiO$_2$/CNTs, due to the robust interaction between TiO_2 and CNTs which is stronger than in Pt on CNTs [82].
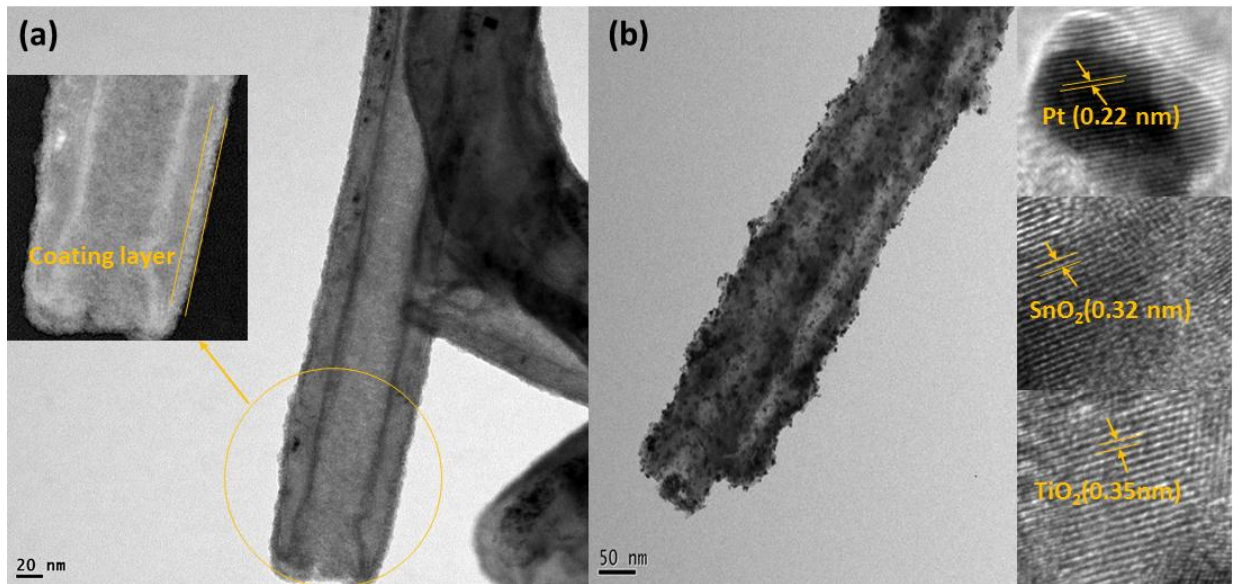

Figure 11. TEM images: (a) well coated CNTs by C-TiO$_2$ without aggregation; (b) Pt distributed (dark spots) on SnO$_2$-C-TiO$_2$/CNTs and the lattice spacing of each element (inset).
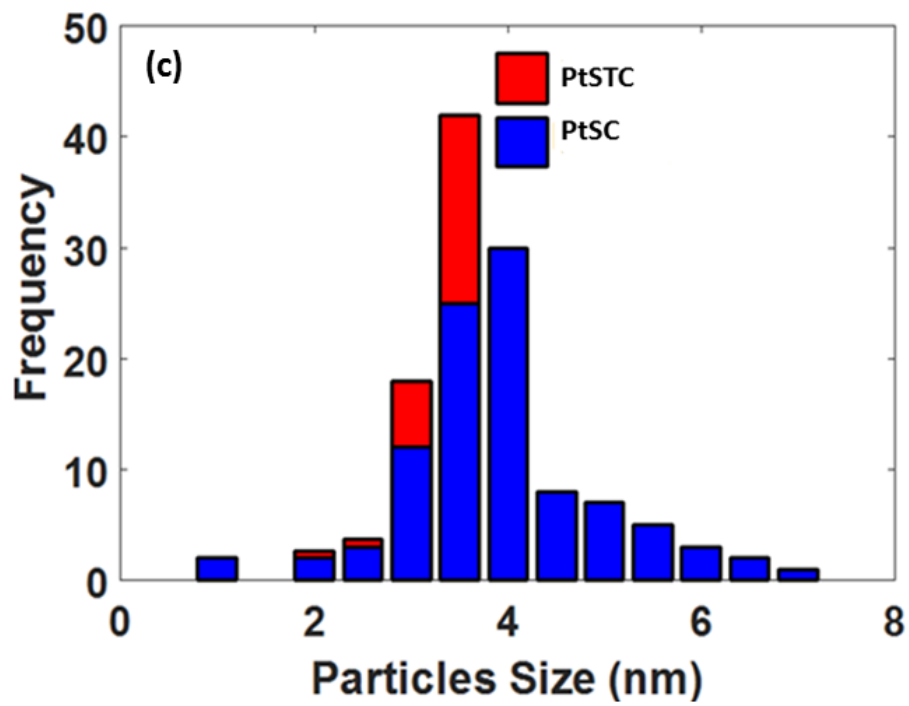
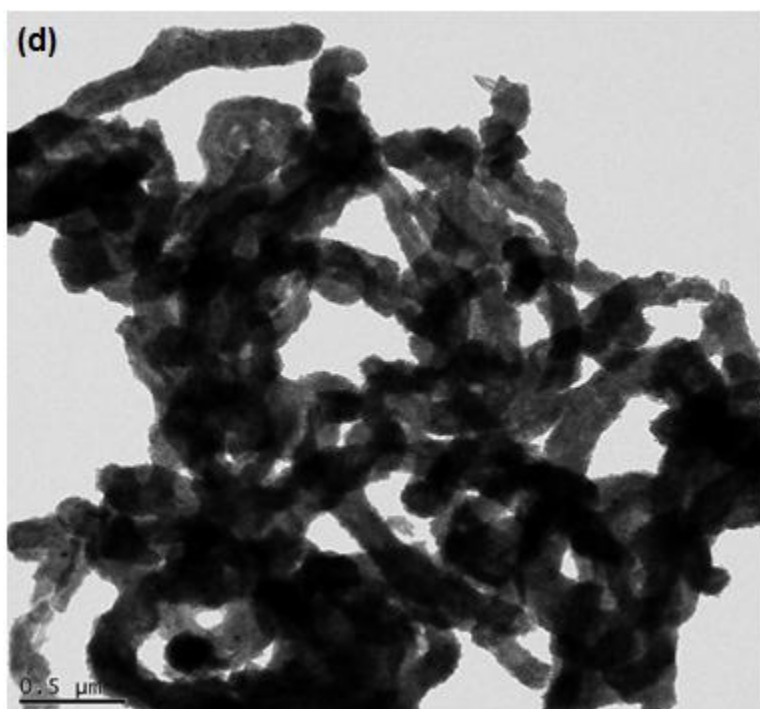Fig 11. (c) Histogram of particles sizes

Fig 11. (d) low resolution TEM image for group of CNTs

The Pt and SnO$_2$ particles were uniformly loaded on the TiO$_2$/CNTs surface due to strong interactions between the metal and the oxides [83]. The Pt, TiO$_2$, and SnO$_2$ were identified by the lattice spacing in the inset, and were found to be 0.22, 0.35, and 0.32 nm, respectively [84]. The morphological character of is revealed in more details in Figure 11b. The particle size, calculated by Bragg's law and PtSTC displayed in Figure 11c shows that the size of the Pt particles in the presence of the double oxides is smaller than that in the catalyst containing only SnO$_2$. In Figure 11d, a group of CNTs coated by titanium dioxide without any bare surface left. Figure 12 shows the XRD patterns of CNTs, PtSTC and PtSC. Diffraction peaks of CNTs at 26°, 42°, 53° and 77° were identified. They matched with the literature corresponding to planes of hexagonal of the graphitic structure [85]. The PtSTC and PtSC exhibited similar results except at 54°, which can be attributed to TiO$_2$ sub-oxides [86]. The peaks in the catalysts at diffraction angles 26.7°, 34°, 38° and 52° were indexed to crystal plane (110), (101), (200) and (211), respectively. The diffraction of peaks at 39.9°, 46.6°, 67.8°, 81.5°, and 86° refers to Pt (111), (200), (220), (311) and (222), respectively. By combining the TEM and XRD data, it can be inferred that the presence of the two oxides enhanced the dispersion of Pt and reduced the particle size as well. Both oxides may act as a catalyst for the growth of Pt nanoparticles in the direction of the Pt (111) crystallographic plane, which is the most stable plane and active surface in methanol electro-oxidation. It was reported that incorporating some transition metal oxide such MnO$_X$ with Pt could enhance the growth of platinum nanoparticles in the direction of Pt (1 1 1) crystallographic plane [87]. In this particular case, the oxides could be considered as a sort of ligands [88].
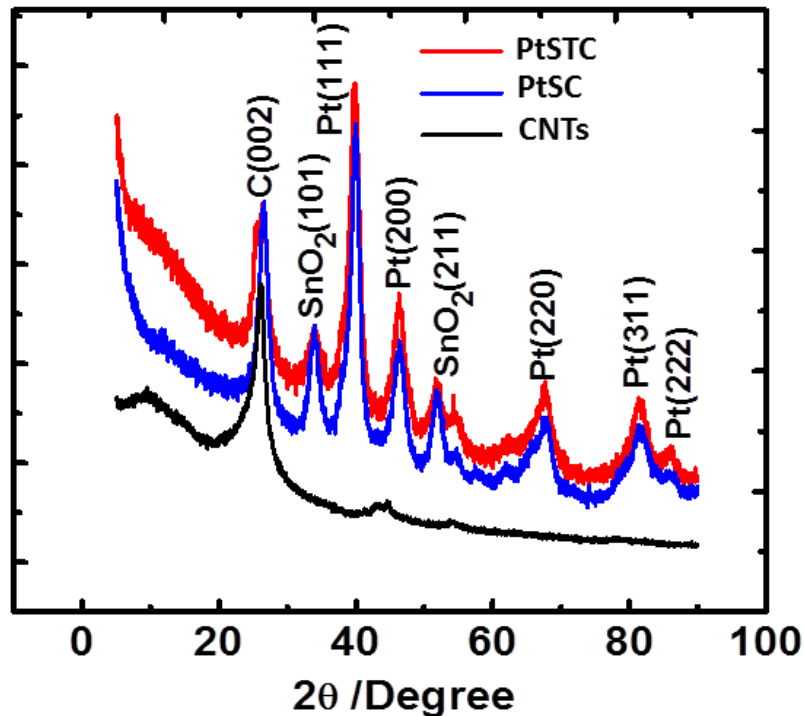
Figure 12. XRD pattern for the two catalysts, and CNTs.

3.2 Electrochemical results

The cyclic voltammograms (CVs) for the catalysts are present in Figure 13. As shown

in Figure 13, the presence of the two oxides enhanced the Pt bonding interaction within the

PtSTC catalyst significantly. The Pt adsorption/desorption peaks are much higher in this

catalyst than in the two others with one without TiO_2 and one without oxides at all. The

relatively flat CV curve positive of -0.05 V for PtSTC is remarkably pronounced. This is

an indication of the resistance to oxidation of the Pt when the support has C-doped TiO_2,

together with SnO_2. This can be attributed to a back donation of electrons from Pt to the

two oxides, making Pt more electronegative, which can be also observed from the XPS

studies presented below. This stability was confirmed by the absence of surface oxidation

in the Pt metal itself. The reduction peak at ca. 0.6 V is attributed to reduction of SnO_2.

The reduction peak at +0.05 V is attributed to hydrogen adsorption on the catalyst.

33
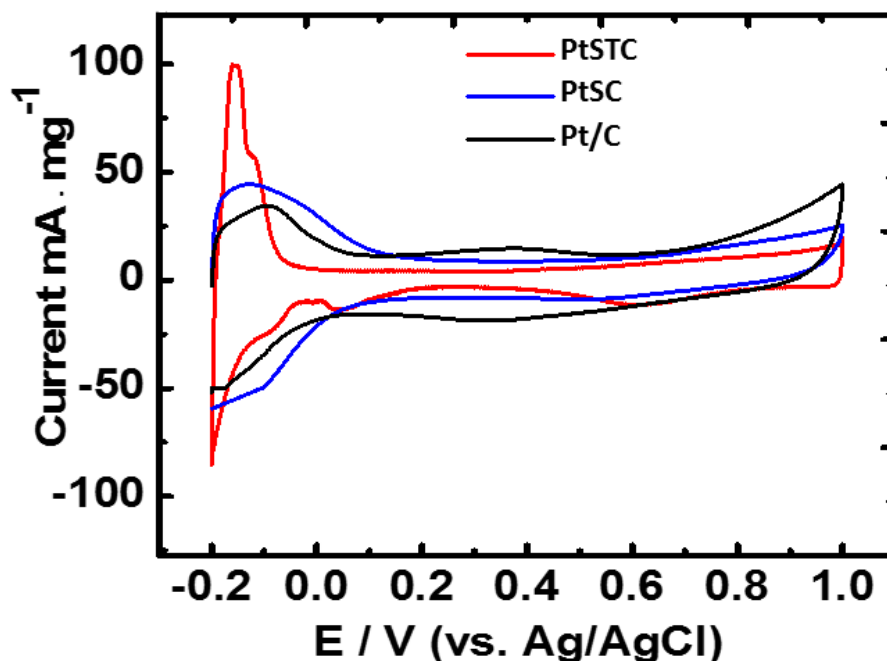
Figure 13. Cyclic voltammetry of the catalysts in $1.0M H_2SO_4$ at scan rate 0.03 V/s.

In the other two catalysts there were rising peaks at high potentials, attributed to the lowering of the electronic Fermi level of the electrode, leading to water reaction with the positive accumulated charge close to the electrode surface forming Pt-O_X [89]. Xu *et al.*, found the activation energy of Pt-Ox dissociation to be 0.77 eV at 25% ML coverage [90]. Adzic's group suggested that most of the Pt-skin surfaces should have an intermediate value of such energy, providing a compromise between the ability to dissociate O_2 and preventing poisoning of the surface with oxygenated intermediates or products [91]. Hydrogen evolution could be determined and compared from Figure 13 as well. The prepared catalyst exhibited less hydrogen desorption potential which refers to the ability of the catalyst to oxidize CO at an early potential. In addition, the early hydrogen adsorption-desorption could be assigned to changing in the crystal face structure of the prepared catalyst as reported. Methanol oxidation on these catalysts is shown in Figure 14a. The

highest activity was found in PtSTC s in the electro-oxidation of methanol. The peak

potentials significantly shifted negatively, and the onset potential was reduced as well. The

shift in the potential peak of methanol oxidation can be explained by reduced interaction

between poisoning species and the Pt catalyst, since the latter had already shared some of

the valence electrons with the oxides. First, the forward scan peak referred to strongly

adsorbed CO oxidation since the CO binds very strongly by 5σ and $2\pi^*$ bonds with the

metals [92]. The required potential for oxidizing chemisorbed species of CO_{ads} was 0.62V.

However, the backward peak at 0.38V indicated a weakly adsorbed, non-oxidized species

such as formic acid or formaldehyde [93]. The dehydrogenation step of methanol to yield

CO starts at low potential; however, other species were formed in the high voltage range

[94]. As a result, it can be presumed that the two oxides made remarkable changes in the

electronic state of Pt [95].
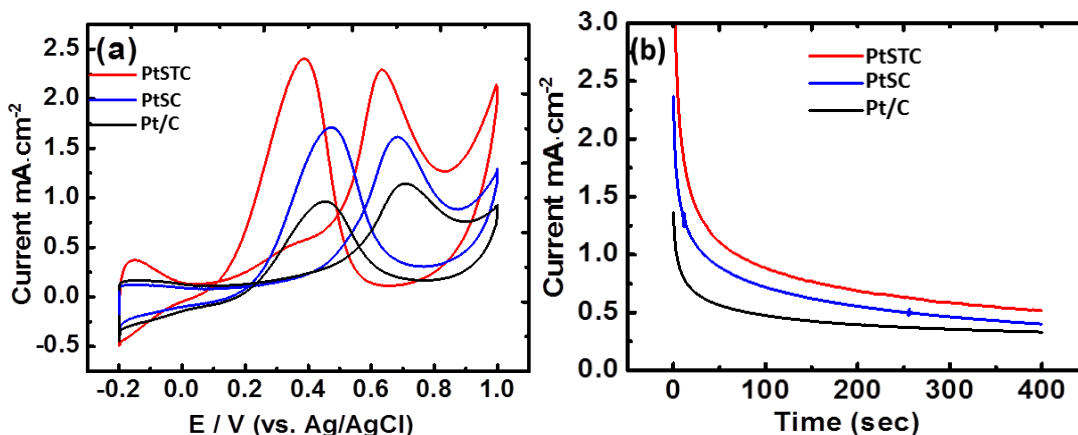
Figure 14. (a) Cyclic voltammetry of the three catalysts at scan rate 30mV s^{-1} in 1.0M CH$_3$OH and 1.0M H$_2$SO$_4$, (b) i-t
curve at 0.7V in1.0M CH$_3$OH and 1.0M H$_2$SO$_4$ electrolyte solution.

The oxides, tin oxide in particular, introduced large enough amounts of OH groups that

donate two electrons to convert CO to CO_2 [96]. Janik and Neurock calculated the barrier

of the reaction of OH and CO on Pt (111) surface, which was 0.5 eV. However, they found

the reaction of CO and O has a higher energy than that between CO and OH [97]. This corroborates with the bifunctional mechanism that the CO is oxidized OH on the SnO_2 at lower potentials, making the Pt catalyst on the double oxide support more durable, as shown in Figure13 (b). The PtSTC were the most durable, giving 140% higher activity than the PtSC and more than 280% of Pt/C. The durable performance is a result of the double oxide support, interacting with the metal catalyst [98]. Figure 15 shows the CV results of the initial cycling and that after 1000 cycles for the PtSTC catalyst. The PtSTC loses 11% in ECSA. Often at high potential, the platinum surface is strongly oxidized by O-species such as OH from water to form Pt-OH at 0.6-0.9V as reported by Conway *et al*. [99]. Therefore, the $Pt-O_X$ decreases the active sites of the catalyst by forming a monolayer [100] of chemisorbed O as observed in the E-TEK catalyst and less observed in the single oxide support in PtSC.

Table 3.Shows the ECSA, current density and potential positions of PtSTC, PtSC, and Pt/C.

Catalyst	ECSA (m^2/g-Pt)	Onset peak (V)	I$_f$ (mA/cm^2)	Peak I$_f$ Potential (V)	I$_b$ (mA/cm^2)	Peak I$_b$ Potential (V)
PtSTC	46	0.11	2.3	0.62	2.4	0.38
PtSC	39	0.36	1.87	0.68	1.98	0.47
Pt/C	34	0.38	1.3	0.70	0.95	0.45
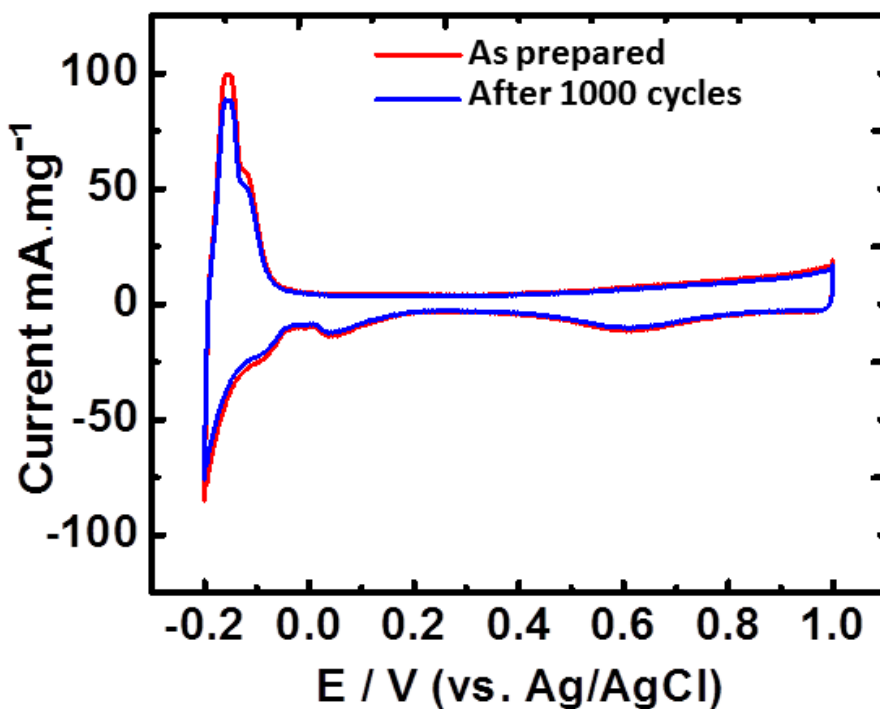
Figure 15. Cyclic voltammetry at scan rate 30mV s^{-1} in 1.0M 1.0MH$_2$SO$_4$ before and after 1000 cycles.

In the case of double oxide support, the Pt-Ox formation was almost eliminated even at high potentials due to the SnO$_2$ coupling with TiO$_2$ as support. According to the *d*-band theory, the binding energy of an adsorbate to a metal surface is largely dependent on the electronic structure of the surface itself [101]. The rich oxide surface increases the anti-bonding level (d-σ)* and lowers the *d*-band center (E$_f$) [102], which makes a weak interaction between the metal and the adsorbate. ESCA obtained by integration of the adsorption–desorption of hydrogen underpotential region after double layer correction is listed in Table 3 above.

3.3 X-Ray photoelectron microscopy results

Figure 15(a) illustrates that the Pt4f $_{7/2}$ binding energy in PtSC was observed 71.6 eV, and it was identical with that reported previously [103]. However, it was shifted in PtSTC to 72.0 eV.
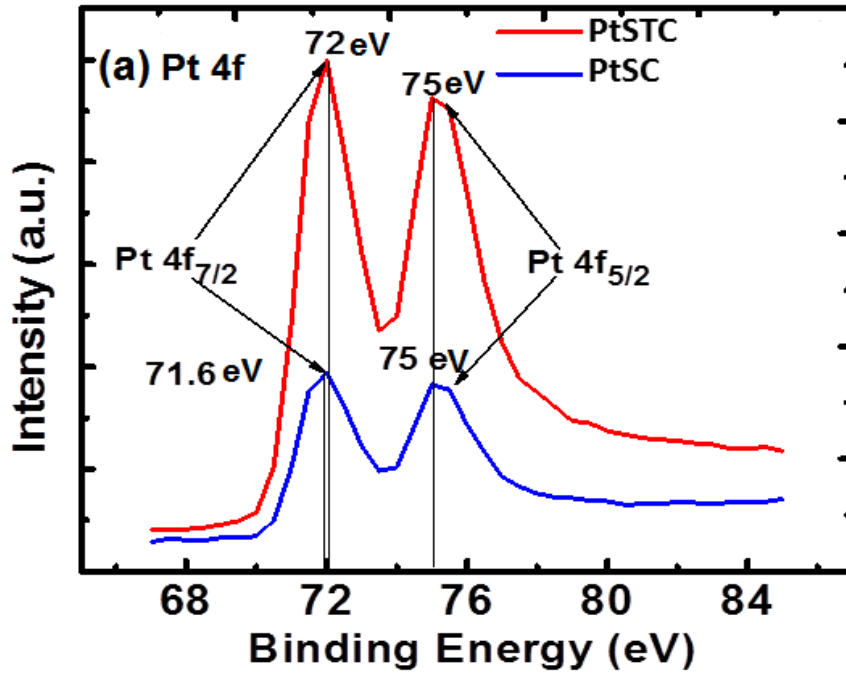
Figure 16. XPS spectra for catalysts, (a) reveals the increasing of binding energy at presence of Titanium dioxide with tin oxide which is strong evidence that Pt electronic state was changed.

The difference was 0.4 eV (corresponding to 38.59 kJ/mole), which reduced the activation barrier of the reaction of the CO with OH on the Pt over layer [104]. Binding energy increases as the oxidation state becomes more positive, implying more stability of the prepared catalyst rather than sharing with poisoning adsorbates [105]. In addition, high binding energy refers to a high CO-tolerance catalyst that could oxidize the CO-like groups at low potentials [106]. The electronic effect can be understood on the basis of the d-band shift model. Flow of electrons occurred from Pt to TiO$_2$ as a back donation electron [107]. Probably, the calcinations of the SnO$_2$-C-TiO$_2$/CNTs at elevated temperatures increased

the level of SnO_2 concentration. Thereby, the high concentration of SnO_2 could lead to high Pt concentration due to the presence of Pt-Sn bond. The 600 °C calcination facilitates the crystal perfection of tin oxide; however, some of the SnO_2 particles may disengage from the surface [108]. Apparently, the presence of both oxides could lead to altering the center of gravity of the d-band regarding to the Fermi level in order to sustain constant filling of the d-band of Pt [109]. Such change is achieved by lowering the d-band center by modifying the electronic and inducing a degree of irregularity in the Pt lattice that makes oxygen species bind more weakly. A higher binding energy of Pt with the support SnO_2-C-TiO_2/CNTs would decrease the binding energy of adsorbates. The evidence for that is the early onset potential and early oxidation peak position in methanol oxidation.

The latter observation can be explained as a different behavior in the methanol oxidation mechanism. In the PtSTC, the forward peak potential refers to strongly adsorbed species oxidation such as carbon monoxide to carbon dioxide as well as the formation of formic acid [110]. The backward low potential might be attributed to formic acid oxidation since the HCOOH has two oxygen atoms. However, other catalysts show positive potential shifting in forward scan that refers to a higher potential required to oxidize the adsorbates. The other catalytic mechanism is to form formaldehyde groups rather than formic acid or the complete dehydrogenation of methanol. Therefore, the presence of tin oxide with titanium dioxide enhanced the complete path of methanol oxidation reaction and promoted the kinetics.

Figure 16 (b) shows the binding energy in high resolution spectra for Sn 3d. All peaks refer to the oxide form of Sn in either Sn (II) or Sn (IV) form which matched the XRD analysis; no metallic tin was detected.
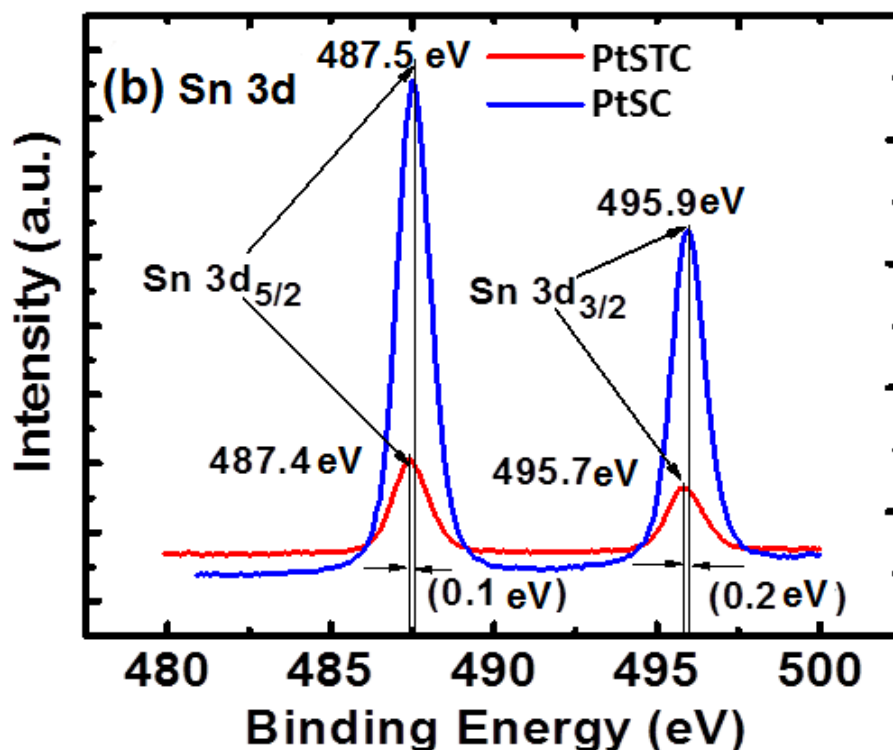
Figure 16. (b) depicts binding energy of tin oxide increased by (0.1eV)

The PtSTC Sn XPS spectra depicts the binding energy Sn 3d $_{5/2}$ and Sn 3d $_{3/2}$ at 487.4 eV and 495.7 eV respectively. On the other hand, the PtSC shows BEs at 487.5 eV and 495.9 eV. The binding energy of the pristine SnO_2 as reported in both oxidized forms are 487.2 ev and 495.5 eV [111]. The shift of Sn BEs in PtSC is higher than in PtSTC. It could be assigned that Sn shared more electrons with the CNTs and Pt. However, in PtSTC, the coating agent reduced the Sn BEs. This could be explained with two reasons. First, Pt bonded with SnO_2 and TiO_2 simultaneously but in different strength degrees, but Pt gives electron back donation to tin oxide. Second, there could be electron sharing between the two oxides for a certain extent as well as with Pt. Figure 16 (c) shows the chemical state of Ti. According to previous report, pure TiO_2 displays BEs at 464.2 eV and 458.5 eV [112].

However, it was suggested the shifting in Ti2p from defect free TiO_2 is caused by surface oxygen vacancy defects [113].
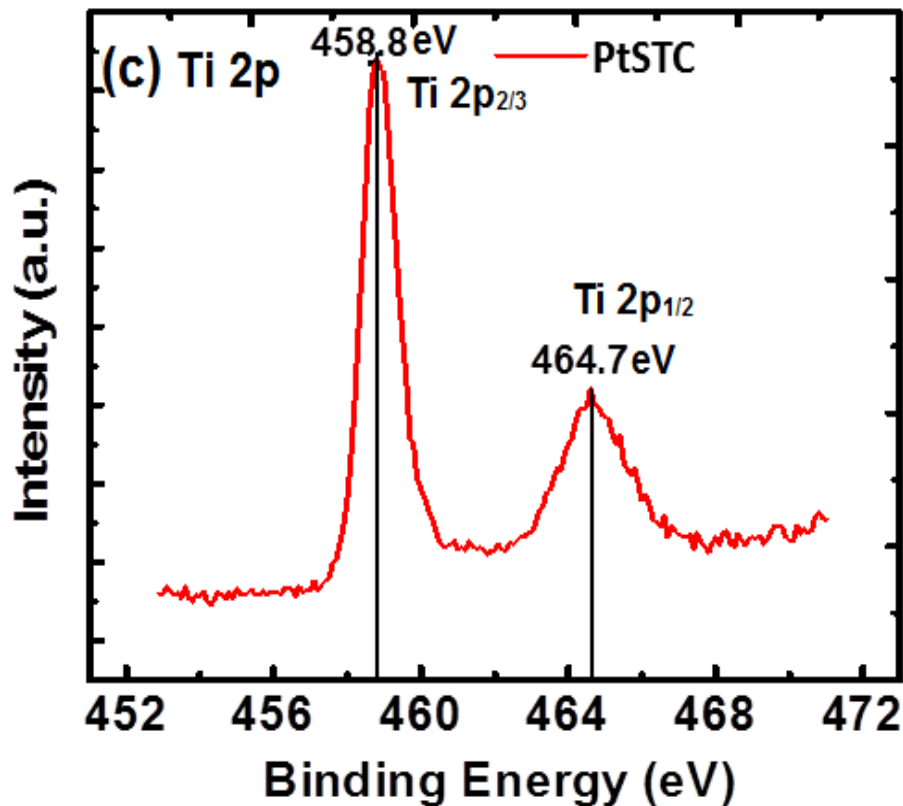
Figure 16. (c) shows Ti 2p ½ and Ti 2p 3/2.

Incorporated carbon could substitute oxygen, which can have a synergistic effect with oxygen vacancies leading to change in the electron structure [114]. Therefore, in the prepared catalyst, the BEs of Ti $2p_{1/2}$ and Ti $2p_{3/2}$ were found to be 464.7 eV and 458.8 eV, respectively. The latter observation can be attributed to partially reduced Ti compared with the Magneli phase Ti_4O_7 which shows BEs at 464.7 eV and 459 eV leading to an improvement in titania electric conductivity [115]. As shown in Figure 16 (d), the binding energy of O 1s in Pt-SnO$_2$/CNTs was 531.3 eV, which was completely consistent with the value reported previously [116]. However, the double oxide support catalyst shows two

peaks of O 1s BE, one at 531.3 eV which refers to SnO_2 and at 530.1 eV which indicates to TiO_2 [117]. This may be attributed to less Pt-Ox groups available as observed in the CVs described above [118]. In addition, oxide coating reduced the oxygen binding energies by shifting them to lower values that could increase the oxide conductivity as observed in Hahn's work [119]. Figure 16 (e) shows that the binding energy of C 1s was 284.7 eV in PtSTC and was 285 eV in PtSC which corresponds to graphite [120]. The difference (0.3 eV) between them could be attributed to the TiO_2 presence with SnO_2 reveals high degree of carbon crystallite state which can provide a more stable electrochemical environment for Pt particles. Moreover, no peaks were noted above 285 eV, due to the absence of carbonate species [121]. Also, at 281 eV there was not a detected peak, which indicates no TiC structure was formed [122].

Figure 16. (d) shows the difference of oxygen bonding group with each catalyst referring to less Pt-Ox group on the platinum. (e) XPS spectra of C 1s.

CHAPTER 4. Conclusions and Future Work

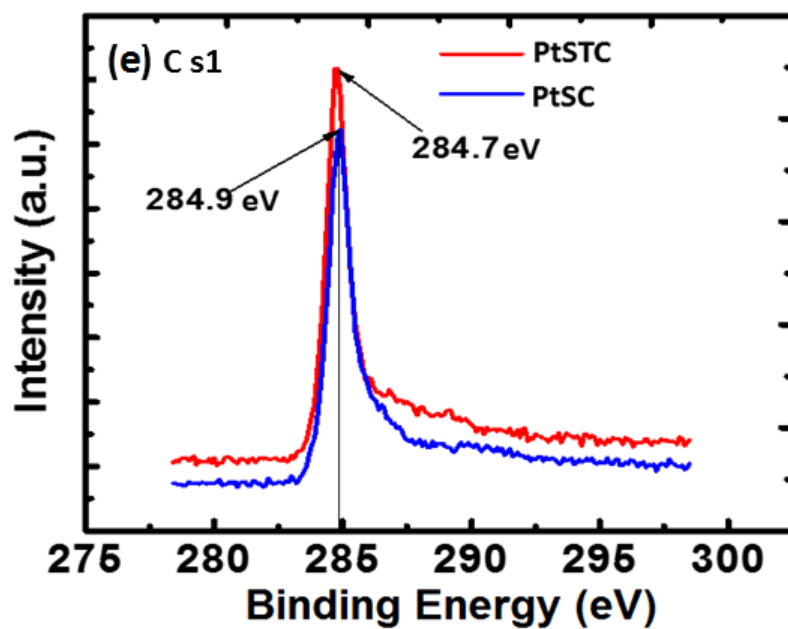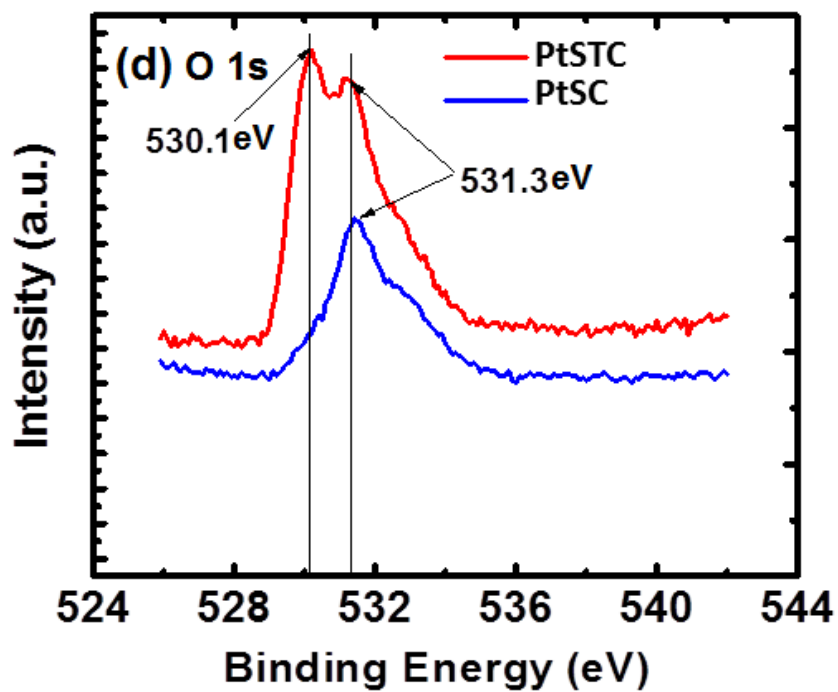As reported in the previous catalyst literature and for all carbon materials including carbon black, graphene and carbon nanotubes as a catalyst support, the mono metal catalyst shows low activity, durability and stability. In addition, incorporation of other noble metals with Pt makes the catalyst non-practical in terms of commercial feasibility. Therefore, it could be concluded that the existence of non-noble metal oxides on the carbon material surface improved the catalyst activity, stability, and durability in the long term. In our work, C-TiO_2/CNTs coated and doped layers were prepared by a sol-gel process and acetylene-decomposition at 700C°, successively. Tin oxide was incorporated at the presence of C-TiO_2/CNTs by hydrolysis of tin dihydrochloride at 70 °C in aqueous solutions. Then, Pt was deposited onto SnO_2-C-TiO_2/CNTs in a polyol process. The catalyst exhibited remarkable methanol oxidation activity of 2.4 mA/cm^2, good durability, and high ECSA. Shifting in potential toward the negative region was observed   and early onset was displayed as well. No Pt surface metal oxidation appeared at high potential due to the back donation of electrons of the platinum to the oxide support. XPS revealed an increase in binding energy of Pt by 0.4 eV, when the coating layer was present. The BE difference (38.59 kJ/mole) decreased the activation energy to oxidize the carbon monoxide, which took place at 0.62 V. Therefore, it can be stated that the key factor was the double oxide support of tin oxide on TiO_2 coated CNTs. From our research results and from literature review presented, we can state that any deposition of platinum on bare carbon material is wasteful of the precious metal. Also, platinum loading on the bare metal oxide is not active regarding the efficiency due to less surface area and less conductivity compared with the carbon material supports. So for the future work, we suggest that intensive efforts are necessary to combine the metal oxides with carbon material in the following way: 1)

modify the topography of the metal oxide by increasing the surface area and porosity such as make a mesoporous and conductive coating., and 2) increase the metal oxide conductivity by elemental doping or change its phase to a Magneli phase.

References

[1] Grove, William Robert, XXIV. on voltaic series and the combination of gases by platinum, *The London and Edinburgh philosophical magazine and journal of science*, 86 (1839) 127-130.

[2] Wang, Dawei, Yang Liu, Jianshe Huang, and Tianyan You, In situ synthesis of Pt/carbon nanofiber nanocomposites with enhanced electrocatalytic activity toward methanol oxidation, *Journal of colloid and interface science*,1 (2012) 199-203.

[3] Oetjen, H-F., V. M. Schmidt, U. Stimming, and F. Trila, Performance data of a proton exchange membrane fuel cell using H 2/CO as fuel gas, *Journal of the Electrochemical Society*,12 (1996) 3838-3842.

[4] Bock, Christina, Chantal Paquet, Martin Couillard, Gianluigi A. Botton, and Barry R. MacDougall, Size-selected synthesis of PtRu nano-catalysts: reaction and size control mechanism, *Journal of the American Chemical Society*, 25 (2004) 8028-8037.

[5] Iwasita, Teresa, Electrocatalysis of methanol oxidation, *Electrochimica Acta*, 22 (2002) 3663-3674.

[6] Li, Xingwei, Jiadi Wei, Yuzheng Chai, and Shuo Zhang, Carbon nanotubes/tin oxide nanocomposite-supported Pt catalysts for methanol electro-oxidation, *Journal of colloid and interface science,* 450 (2015) 74-81.

[7] Wei, Jiadi, Qingjun Guo, Xingwei Li, and Bing Li, Molten salts synthesis of tin dioxide/nitrogen-doped carbon composite as Pt catalyst support for methanol electro-oxidation, *Journal of Materials Science*,14 (2015) 4952-4961.

[8] Hu, Chuangang, Yanxia Cao, Lin Yang, Zhengyu Bai, Yuming Guo, Kui Wang, and Pengle Xu, Preparation of highly dispersed Pt-SnO x nanoparticles supported on multi-walled carbon nanotubes for methanol oxidation, *Applied Surface Science* 257, 18 (2011) 7968-7974.

[9] Sasaki, Kotaro, Nebojsa Marinkovic, Hugh S. Isaacs, and Radoslav R. Adzic, Synchrotron-Based in Situ Characterization of Carbon-Supported Platinum and Platinum Monolayer Electrocatalysts, *ACS Catalysis*, 1 (2015) 69-76.

[10] Zhao, Guang-Yu, and Hu-Lin Li, Electrochemical oxidation of methanol on Pt nanoparticles composited MnO 2 nanowire arrayed electrode, *Applied Surface Science*, 10 (2008) 3232-3235.

[11] Antolini, E., J. R. C. Salgado, and E. R. Gonzalez, Carbon supported Pt75M25 (M= Co, Ni) alloys as anode and cathode electrocatalysts for direct methanol fuel cells, *Journal of Electroanalytical Chemistry*, 1 (2005) 145-154.

[12] Zhao, Yanchun, Xiulin Yang, and Jianniao Tian, Electrocatalytic oxidation of methanol at 2-aminophenoxazin-3-one-functionalized multiwalled carbon nanotubes supported PtRu nanoparticles, *Electrochimica Acta*, 27 (2009) 7114-7120.

[13] Xu, J. B., and T. S. Zhao, Synthesis of well-dispersed Pt/carbon nanotubes catalyst using dimethylformamide as a cross-link, *Journal of power sources*, 4 (2010) 1071-1075.

[14] Jerkiewicz, Gregory, Gholamreza Vatankhah, Jean Lessard, Manuel P. Soriaga, and Yeon-Su Park, Surface-oxide growth at platinum electrodes in aqueous H 2 SO 4: Reexamination of its mechanism through combined cyclic-voltammetry,

electrochemical quartz-crystal nanobalance, and Auger electron spectroscopy measurements, *Electrochimica Acta*, 9 (2004) 1451-1459.

[15] Ghenciu, Anca Faur, Review of fuel processing catalysts for hydrogen production in PEM fuel cell systems, *Current opinion in solid state and materials science*, (2002) 389-399.

[16] Song, Chunshan, Fuel processing for low-temperature and high-temperature fuel cells: Challenges, and opportunities for sustainable development in the 21st century, *Catalysis today*, 1 (2002) 17-49.

[17] Lu, G-Q., W. Chrzanowski, and A. Wieckowski, Catalytic methanol decomposition pathways on a platinum electrode, The Journal of Physical Chemistry B, 23 (2000) 5566-5572.

[18] Rolison, Debra R., Patrick L. Hagans, Karen E. Swider, and Jeffrey W. Long, Role of hydrous ruthenium oxide in Pt-Ru direct methanol fuel cell anode electrocatalysts: the importance of mixed electron/proton conductivity, *Langmuir*, 3 (1999) 774-779.

[19] Farmer, Jason A., and Charles T. Campbell, Ceria maintains smaller metal catalyst particles by strong metal-support bonding, *Science*, 5994 (2010) 933-936.

[20] Park, Kyung-Won, Jong-Ho Choi, Boo-Kil Kwon, Seol-Ah Lee, Yung-Eun Sung, Heung-Yong Ha, Seong-Ahn Hong, Hongsun Kim, and Andrzej Wieckowski, Chemical and electronic effects of Ni in Pt/Ni and Pt/Ru/Ni alloy nanoparticles in methanol electrooxidation, *The Journal of Physical Chemistry B*, 8 (2002) 1869-1877.

[21] Wang, Ai-Qin, Chun-Ming Chang, and Chung-Yuan Mou, Evolution of catalytic activity of Au-Ag bimetallic nanoparticles on mesoporous support for CO oxidation,*The Journal of Physical Chemistry B*, 40 (2005) 18860-18867.

[22] Zhang, Yawen, Wenyu Huang, Susan E. Habas, John N. Kuhn, Michael E. Grass, Yusuke Yamada, Peidong Yang, and Gabor A. Somorjai, Near-Monodisperse Ni−Cu Bimetallic Nanocrystals of Variable Composition: Controlled Synthesis and Catalytic Activity for H2 Generation, *The Journal of Physical Chemistry C*, 32 (2008) 12092-12095.

[23] Shao, Yuyan, Geping Yin, and Yunzhi Gao, Understanding and approaches for the durability issues of Pt-based catalysts for PEM fuel cell, *Journal of Power Sources*, 2 (2007) 558-566.

[24] Gasteiger, Hubert A., Shyam S. Kocha, Bhaskar Sompalli, and Frederick T. Wagner, Activity benchmarks and requirements for Pt, Pt-alloy, and non-Pt oxygen reduction catalysts for PEMFCs, *Applied Catalysis B: Environmental*, 1 (2005) 9-35.

[25] Chen, Xiaobo, and Samuel S. Mao, Titanium dioxide nanomaterials: synthesis, properties, modifications, and applications, *Chem. Rev*, 7 (2007) 2891-2959.

[26] Lee, S-H., Rohit Deshpande, Phil A. Parilla, Kim M. Jones, Bobby To, A. Harv Mahan, and Anne C. Dillon, Crystalline WO3 nanoparticles for highly improved electrochromic applications, *Advanced Materials*, 6 (2006) 763-766.

[27] Zhou, Jigang, Xingtai Zhou, Xuhui Sun, Ruying Li, Michael Murphy, Zhifeng Ding, Xueliang Sun, and Tsun-Kong Sham, Interaction between Pt nanoparticles and carbon nanotubes–An X-ray absorption near edge structures (XANES) study, *Chemical physics letters*, 4 (2007) 229-232.

[28] Lee, Jinwoo, Jaeyun Kim, and Taeghwan Hyeon, Recent progress in the synthesis of porous carbon materials, *Advanced Materials*,16 (2006) 2073-2094.

[29] Cui, Xiangzhi, Jianlin Shi, Lingxia Zhang, Meiling Ruan, and Jianhua Gao, PtCo supported on ordered mesoporous carbon as an electrode catalyst for methanol oxidation, 1 (2009) 186-194.

[30] Su, Fabing, Jianhuang Zeng, Xiaoying Bao, Yaoshan Yu, Jim Yang Lee, and X. S. Zhao, Preparation and characterization of highly ordered graphitic mesoporous carbon as a Pt catalyst support for direct methanol fuel cells, *Chemistry of materials*, 15 (2005) 3960-3967.

[31] Chai, Geun Seok, Suk Bon Yoon, Jong-Sung Yu, Jong-Ho Choi, and Yung-Eun Sung, Ordered porous carbons with tunable pore sizes as catalyst supports in direct methanol fuel cell, *The Journal of Physical Chemistry B*, 22 (2004) 7074-7079.

[32] Cui, Xiangzhi, Fangming Cui, Qianjun He, Limin Guo, Meiling Ruan, and Jianlin Shi, Graphitized mesoporous carbon supported Pt–SnO 2 nanoparticles as a catalyst for methanol oxidation, *Fuel*, 2 (2010) 372-377.

[33] Yu, Jong-Sung, Soonki Kang, Suk Bon Yoon, and Geunseok Chai, Fabrication of ordered uniform porous carbon networks and their application to a catalyst supporter, *Journal of the American Chemical Society*, 32 (2002) 9382-9383.

[34] Cui, Xiangzhi, Fangming Cui, Qianjun He, Limin Guo, Meiling Ruan, and Jianlin Sh, Graphitized mesoporous carbon supported Pt–SnO 2 nanoparticles as a catalyst for methanol oxidation, *Fuel*, 2 (2010) 372-377.

[35] Shao, Yuyan, Geping Yin, and Yunzhi Gao, Understanding and approaches for the durability issues of Pt-based catalysts for PEM fuel cell, *Journal of Power Sources*, 2 (2007) 558-566.

[36] Thess, Andreas, Roland Lee, Pavel Nikolaev, and Hongjie Dai, Crystalline ropes of metallic carbon nanotubes, *Science*, 5274 (1996) 483.

[37] Lin, Yu-Hung, Yang-Chih Hsueh, Po-Sheng Lee, Chih-Chieh Wang, Jyh Ming Wu, Tsong-Pyng Perng, and Han C. Shih, Fabrication of tin dioxide nanowires with ultrahigh gas sensitivity by atomic layer deposition of platinum, *Journal of Materials Chemistry*, 28 (2011) 10552-10558.

[38] Luo, Fan, Shijun Liao, Dai Dang, Yan Zheng, Dongwei Xu, Haoxiong Nan, Ting Shu, and Zhiyong Fu, Tin and silicon binary oxide on the carbon support of a Pt electrocatalyst with enhanced activity and durability, *ACS Catalysis*, 4 (2015) 2242-2249.

[39] Novoselov, Kostya S., Andre K. Geim, Sergei V. Morozov, D. Jiang, Y_ Zhang, Sergey V. Dubonos, Irina V. Grigorieva, and Alexandr A. Firsov, Electric field effect in atomically thin carbon films, *Science*, 5696 (2004) 666-669.

[40] Geim, Andre K., and Konstantin S. Novoselov, The rise of graphene, *Nature materials*, 3 (2007) 183-191.

[41] Peigney, Alain, Ch Laurent, Emmanuel Flahaut, R. R. Bacsa, and Abel Rousset, Specific surface area of carbon nanotubes and bundles of carbon nanotubes, *Carbon*, 4 (2001) 507-514.

[42] Zhang, Yuanbo, Yan-Wen Tan, Horst L. Stormer, and Philip Kim, Experimental observation of the quantum Hall effect and Berry's phase in graphene, *Nature*, 7065 (2005) 201-204.

[43] Allen, Matthew J., Vincent C. Tung, and Richard B. Kaner, Honeycomb carbon: a review of graphene, *Chemical reviews*, 1 (2009) 132-145.

[44] Dikin, Dmitriy A., Sasha Stankovich, Eric J. Zimney, Richard D. Piner, Geoffrey HB Dommett, Guennadi Evmenenko, SonBinh T. Nguyen, and Rodney S. Ruoff, Preparation and characterization of graphene oxide paper, *Nature*, 7152 (2007) 457-460.

[45] Li, Wenzhen, Changhai Liang, Weijiang Zhou, Jieshan Qiu, Zhenhua Zhou, Gongquan Sun, and Qin Xin, Preparation and characterization of multiwalled carbon nanotube-supported platinum for cathode catalysts of direct methanol fuel cells, *The Journal of Physical Chemistry B*, 26 (2003) 6292-6299.

[46] Balbuena, Perla B., Diego Altomare, Nagendra Vadlamani, Sridhar Bingi, Luis A. Agapito, and Jorge M. Seminario, Adsorption of O, OH, and H2O on Pt-based bimetallic clusters alloyed with Co, Cr, and Ni, *The Journal of Physical Chemistry A*, 30 (2004) 6378-6384.

[47] Kou, Rong, Yuyan Shao, Donghai Wang, Mark H. Engelhard, Ja Hun Kwak, Jun Wang, Vilayanur V. Viswanathan et al, Enhanced activity and stability of Pt catalysts on functionalized graphene sheets for electrocatalytic oxygen reduction, *Electrochemistry Communications*, 5 (2009) 954-957.

[48] Li, Yueming, Longhua Tang, and Jinghong Li, Preparation and electrochemical performance for methanol oxidation of Pt/graphene nanocomposites, *Electrochemistry Communications*, 4 (2009) 846-849.

[49] Dong, Lifeng, Raghavendar Reddy Sanganna Gari, Zhou Li, Michael M. Craig, and Shifeng Hou, Graphene-supported platinum and platinum–ruthenium nanoparticles with high electrocatalytic activity for methanol and ethanol oxidation, *Carbon*, 3 (2010) 781-787.

[50] Seger, Brian, and Prashant V. Kamat, Electrocatalytically active graphene-platinum nanocomposites. Role of 2-D carbon support in PEM fuel cells, *The Journal of Physical Chemistry C*, 19 (2009) 7990-7995.

[51] Guo, Shaojun, Shaojun Dong, and Erkang Wang, Three-dimensional Pt-on-Pd bimetallic nanodendrites supported on graphene nanosheet: facile synthesis and used as an advanced nanoelectrocatalyst for methanol oxidation, *ACS nano*, 1 (2009) 547-555.

[52] Cheng, Niancai, Jian Liu, Mohammad Norouzi Banis, Dongsheng Geng, Ruying Li, Siyu Ye, Shanna Knights, and Xueliang Sun, High stability and activity of Pt electrocatalyst on atomic layer deposited metal oxide/nitrogen-doped graphene hybrid support, *international journal of hydrogen energy*, 28 (2014) 15967-15974.

[53] Abdulagatov, Aziz I., Kalvis E. Terauds, Jonathan J. Travis, Andrew S. Cavanagh, Rishi Raj, and Steven M. George, Pyrolysis of titanicone molecular layer deposition films as precursors for conducting TiO2/carbon composite films, *The Journal of Physical Chemistry C*, 34 (2013) 17442-17450.

[54] Iijima, Sumio, and Toshinari Ichihashi, Single-shell carbon nanotubes of 1-nm diameter, (1993) 603-605.

[55] Thess, Andreas, Roland Lee, Pavel Nikolaev, and Hongjie Dai, Crystalline ropes of metallic carbon nanotubes, *Science*, 5274 (1996) 483.

[56] Fanning, Paul E., and M. Albert Vannice, A DRIFTS study of the formation of surface groups on carbon by oxidation, *Carbon*, 5 (1993) 721-730.

[57] Hu, C. G., W. L. Wang, K. J. Liao, G. B. Liu, and Y. T. Wang, Systematic investigation on the properties of carbon nanotube electrodes with different chemical treatments, *Journal of physics and chemistry of solids*, 10 (2004) 1731-1736.

[58] Kleshch, V. I., T. Susi, A. G. Nasibulin, E. D. Obraztsova, A. N. Obraztsov, and E. I. Kauppinen, A comparative study of field emission from NanoBuds, nanographite and pure or N-doped single-wall carbon nanotubes, *physica status solidi (b)*, 11-12 (2010) 3051-3054.

[59] Yu, Kehan, Ganhua Lu, Zheng Bo, Shun Mao, and Junhong Chen,Carbon nanotube with chemically bonded graphene leaves for electronic and optoelectronic applications, *The Journal of Physical Chemistry Letters*, 13 (2011) 1556-1562.

[60] Klink, Stefan, Edgar Ventosa, Wei Xia, Fabio La Mantia, Martin Muhler, and Wolfgang Schuhmann, Tailoring of CNT surface oxygen groups by gas-phase oxidation and its implications for lithium ion batteries, *Electrochemistry Communications,* 1 (2012) 10-13.

[61] Vinke, P., M. Van der Eijk, M. Verbree, A. F. Voskamp, and H. Van Bekkum, Modification of the surfaces of a gasactivated carbon and a chemically activated carbon with nitric acid, hypochlorite, and ammonia, *Carbon*, 4 (1994) 675-686.

[62]Yoon, Byunghoon, Horng-Bin Pan, and Chien M. Wai, Relative catalytic activities of carbon nanotube-supported metallic nanoparticles for room-temperature hydrogenation of benzene, *The Journal of Physical Chemistry C*, 4 (2009) 1520-1525.

[63] Onoe, Takashi, Shinji Iwamoto, and Masashi Inoue, Synthesis and activity of the Pt catalyst supported on CNT, *Catalysis Communications*, 4 (2007) 701-706.

[64] Wu, Shuchang, Guodong Wen, Robert Schlögl, and Dang Sheng Su, Carbon nanotubes oxidized by a green method as efficient metal-free catalysts for nitroarene reduction, *Physical Chemistry Chemical Physics*, 17 (2015) 1567-1571.

[65] Li, Xing, Yongxiao Tuo, Ping Li, Xuezhi Duan, Hao Jiang, and Xinggui Zhou, Effects of carbon support on microwave-assisted catalytic dehydrogenation of decalin, *Carbon,* 67 (2014) 775-783.

[66] Qian, Weizhong, Tang Liu, Fei Wei, Zhanwen Wang, and Hao Yu, Carbon nanotubes containing iron and molybdenum particles as a catalyst for methane decomposition, *Carbon*, 4 (2003) 846-848.

[67] Li, Wenzhen, Changhai Liang, Weijiang Zhou, Jieshan Qiu, Zhenhua Zhou, Gongquan Sun, and Qin Xin, Preparation and characterization of multiwalled carbon nanotube-supported platinum for cathode catalysts of direct methanol fuel cells, *The Journal of Physical Chemistry B*, 26 (2003) 6292-6299.

[68] Marković, Nenad M., Hubert A. Gasteiger, Philip N. Ross, Xudong Jiang, Ignacio Villegas, and Michael J. Weaver, Electro-oxidation mechanisms of methanol and formic acid on Pt-Ru alloy surfaces, *Electrochimica Acta*, 1 (1995) 91-98.

[69] Ticanelli, E., J. G. Beery, M. T. Paffett, and S. Gottesfeld, An electrochemical, ellipsometric, and surface science investigation of the PtRu bulk alloy surface, *Journal of electroanalytical chemistry and interfacial electrochemistry*, 1 (1989) 61-77.

[70] He, Zhibin, Jinhua Chen, Dengyou Liu, Haihui Zhou, and Yafei Kuang, Electrodeposition of Pt–Ru nanoparticles on carbon nanotubes and their

electrocatalytic properties for methanol electrooxidation, *Diamond and Related Materials*, 10 (2004) 1764-1770.

[71] Lamy, C., S. Rousseau, E. M. Belgsir, C. Coutanceau, and J-M. Léger, Recent progress in the direct ethanol fuel cell: development of new platinum–tin electrocatalysts, *Electrochimica Acta*, 22 (2004) 3901-3908.

[72] Lu, C., C. Rice, R. I. Masel, P. K. Babu, P. Waszczuk, H. S. Kim, E. Oldfield, and A. U. H. V. Wieckowski, UHV, electrochemical NMR, and electrochemical studies of platinum/ruthenium fuel cell catalysts, *The Journal of Physical Chemistry B*, 37 (2002) 9581-9589.

[73] Hu, Chuangang, Yanxia Cao, Lin Yang, Zhengyu Bai, Yuming Guo, Kui Wang, and Pengle Xu, Preparation of highly dispersed Pt-SnO x nanoparticles supported on multi-walled carbon nanotubes for methanol oxidation, *Applied Surface Science*, 18 (2011) 7968-7974.

[74] Yan, Litao, Kan Huang, Yougui Chen, and Yangchuan Xing,High content niobium in rutile titania as catalyst support to promote methanol electro-oxidation, *ECS Electrochemistry Letters*, 5 (2014) F27-F29.

[75] Amin, R. S., Amani E. Fetohi, RM Abdel Hameed, and K. M. El-Khatib, Electrocatalytic activity of Pt–ZrO 2 supported on different carbon materials for methanol oxidation in H 2 SO 4 solution, *International Journal of Hydrogen Energy*, 3 (2016) 1846-1858.

[76] Pang, H. L., X. H. Zhang, X. X. Zhong, B. Liu, X. G. Wei, Y. F. Kuang, and J. H. Chen, Preparation of Ru-doped SnO 2-supported Pt catalysts and their electrocatalytic properties for methanol oxidation, *Journal of colloid and interface science*,1 (2008) 193-198.

[77] Dou, Meiling, Ming Hou, Dong Liang, Wangting Lu, Zhigang Shao, and Baolian Yi, SnO 2 nanocluster supported Pt catalyst with high stability for proton exchange membrane fuel cells, *Electrochimica Acta*, 92 (2013) 468-473.

[78] Chen, Chung-Shou, and Fu-Ming Pan, Electrocatalytic activity of Pt nanoparticles deposited on porous TiO 2 supports toward methanol oxidation." *Applied Catalysis B: Environmental*, 3 (2009) 663-669.

[79] Kakati, Nitul, Jatindranath Maiti, Seung Hyun Jee, Seok Hee Lee, and Young Soo Yoon, Hydrothermal synthesis of PtRu on CNT/SnO 2 composite as anode catalyst for methanol oxidation fuel cell, *Journal of Alloys and Compounds*, 18 (2011) 5617-5622.

[80] Song, Huanqiao, Xinping Qiu, and Fushen Li, Effect of heat treatment on the performance of TiO 2-Pt/CNT catalysts for methanol electro-oxidation, *Electrochimica Acta,* 10 (2008) 3708-3713.

[81] Ren, Guoqiang, Synthesis, characterization and application of Pd-Pt bimetallic nanoparticles and carbon nanotubes supported nanocomposites, MS Thesis, Missouri University of Science and Technology, 2007.

[82] Ye, Weichun, Haiyuan Hu, Hong Zhang, Feng Zhou, and Weimin Liu, Multi-walled carbon nanotube supported Pd and Pt nanoparticles with high solution affinity for effective electrocatalysis, *Applied Surface Science*, 22 (2010) 6723-6728.

[83] Yu, Shuping, Qiubo Liu, Wensheng Yang, Kefei Han, Zhongming Wang, and Hong Zhu, Graphene–CeO 2 hybrid support for Pt nanoparticles as potential

electrocatalyst for direct methanol fuel cells, *Electrochimica Acta*, 94 (2013) 245-251.

[84] Zhang, Sheng, Yuyan Shao, Geping Yin, and Yuehe Lin, Carbon nanotubes decorated with Pt nanoparticles via electrostatic self-assembly: a highly active oxygen reduction electrocatalyst, *Journal of Materials Chemistry*, 14 (2010) 2826-2830.

[85] Chetty, Raghuram, Shankhamala Kundu, Wei Xia, Michael Bron, Wolfgang Schuhmann, Valentin Chirila, Waltraut Brandl, Thomas Reinecke, and Martin Muhler, PtRu nanoparticles supported on nitrogen-doped multiwalled carbon nanotubes as catalyst for methanol electrooxidation, *Electrochimica Acta*, 17 (2009) 4208-4215.

[86] Hahn, Robert, Andrei Ghicov, Jarno Salonen, Vesa-Pekka Lehto, and Patrik Schmuki, Carbon doping of self-organized TiO2 nanotube layers by thermal acetylene treatment, *Nanotechnology*, 10 (2007) 105604.

[87] Gong, Xuezhong, Yun Yang, and Shaoming Huang, Mn 3 O 4 catalyzed growth of polycrystalline Pt nanoparticles and single crystalline Pt nanorods with high index facets, *Chemical Communications*, 3 (2011) 1009-1011.

[88] Smith, J. R., F. C. Walsh, and R. L. Clarke, Electrodes based on Magnéli phase titanium oxides: the properties and applications of Ebonex® materials, *Journal of applied electrochemistry*, 10 (1998) 1021-1033.

[89] Xu, Ye, Andrei V. Ruban, and Manos Mavrikakis, Adsorption and dissociation of O2 on Pt-Co and Pt-Fe alloys, *Journal of the American Chemical Society*, 14 (2004) 4717-4725.

[90] Zhang, Junliang, Miomir B. Vukmirovic, Ye Xu, Manos Mavrikakis, and Radoslav R. Adzic, Controlling the Catalytic Activity of Platinum-Monolayer Electrocatalysts for Oxygen Reduction with Different Substrates, *Angewandte Chemie International Edition,* 14 (2005) 2132-2135.

[91] Kita, Hideaki, Shen Ye, and Yunzhi Gao, Mass transfer effect in hydrogen evolution reaction on Pt single-crystal electrodes in acid solution, *Journal of Electroanalytical Chemistry*, 1-2 (1992) 351-357.

[92] Hammer, Bjørk, Y. Morikawa, and Jens Kehlet Nørskov, CO chemisorption at metal surfaces and overlayers, *Physical review letters*, 12 (1996) 2141.

[93] Hari Krishna Charan, P., G. Ranga Rao, and P. Justin, High performance Pt-Nb2O5/C electrocatalysts for methanol electrooxidation in acidic media, *Applied Catalysis B: Environmental*,100(2010) 510-515.

[94] Cao, D., G-Q. Lu, Andrzei Wieckowski, Sally A. Wasileski, and Matthew Neurock, Mechanisms of methanol decomposition on platinum: A combined experimental and ab initio approach, *The Journal of Physical Chemistry B*,23 (2005) 11622-11633.

[95] Siracusano, S., A. Stassi, V. Baglio, A. S. Aricò, F. Capitanio, and A. C. Tavares, Investigation of carbon-supported Pt and PtCo catalysts for oxygen reduction in direct methanol fuel cells, *Electrochimica Acta*, 21 (2009) 4844-4850.

[96] Mukerjee, Sanjeev, and James McBreen, An In Situ X-Ray Absorption Spectroscopy Investigation of the Effect of Sn Additions to Carbon-Supported Pt Electrocatalysts: Part I, *Journal of the Electrochemical Society*,2 (1999) 600-606.

[97] Janik, Michael J., and Matthew Neurock, A first principles analysis of the electro-oxidation of CO over Pt (111), *Electrochimica acta*, 18 (2007) 5517-5528.

[98] Natarajan, Sadesh Kumar, and Jean Hamelin, Electrochemical durability of carbon nanostructures as catalyst support for PEMFCs, *Journal of The Electrochemical Society*, 2 (2009) B210-B215.

[99] Conway, Brian E, Electrochemical oxide film formation at noble metals as a surface-chemical process, *Progress in surface science*,4 (1995) 331-452.

[100] Harrington, David A, Simulation of anodic Pt oxide growth, *Journal of Electroanalytical Chemistry*, 1 (1997) 101-109.

[101] Stamenkovic V, Mun BS, Mayrhofer KJJ, Ross PN, Markovic NM, Rossmeisl J, Greeley J, Norskov JK, *Angew. Chem,* 118 (2006) 2963-2967.

[102] Hammer, B., and J. K. Norskov. Why gold is the noblest of all the metals?, *Nature* 376, no. 6537 (1995): 238-240.

[103] Jusys, Z., J. Kaiser, and R. J. Behm, Methanol electrooxidation over Pt/C fuel cell catalysts: dependence of product yields on catalyst loading, *Langmuir*, 17 (2003) 6759-6769.

[104] Li, Xingwei, Jiadi Wei, Yuzheng Chai, and Shuo Zhang, Carbon nanotubes/tin oxide nanocomposite-supported Pt catalysts for methanol electro-oxidation, *Journal of colloid and interface science* 450 (2015) 74-81.

[105] Saravanan, Chandra, Barry D. Dunietz, Nenad M. Markovic, Gabor A. Somorjai, Phil N. Ross, and Martin Head-Gordon, Electro-oxidation of CO on Pt-based electrodes simulated by electronic structure calculations, *Journal of Electroanalytical Chemistry*, 554 (2003) 459-465.

[106] Douglas, A, Stanley, R, F, James, Principles of instrumental Analysis: Surface characterization, 6th ed., University of Kentucky, (2006) pp 590-591.

[107] Chen, Siguo, Zidong Wei, XueQiang Qi, Lichun Dong, Yu-Guo Guo, Lijun Wan, Zhigang Shao, and Li Li, Nanostructured polyaniline-decorated Pt/C@ PANI core–shell catalyst with enhanced durability and activity, *Journal of the American Chemical Society*, 32 (2012) 13252-13255.

[108] Ge, Q., S. Desai, M. Neurock, and K. Kourtakis, CO adsorption on Pt-Ru surface alloys and on the surface of Pt-Ru bulk alloy, *The Journal of Physical Chemistry B*, 39 (2001) 9533-9536.

[109] Wang, Yankun, Jie Ding, Yanhui Liu, Yushan Liu, Qiang Cai, and Jianmin Zhang ,SnO 2@ reduced graphene oxide composite for high performance lithium-ion battery, *Ceramics International*, 10 (2015) 15145-15152.

[110] Kitchin, John R., Jens Kehlet Nørskov, Mark A. Barteau, and J. G. Chen,Role of strain and ligand effects in the modification of the electronic and chemical properties of bimetallic surfaces, *Physical review letters*,15 (2004) 156801.

[111] Chen, Yan Xia, Atsushi Miki, Shen Ye, Hidetada Sakai, and Masatoshi Osawa Formate, an active intermediate for direct oxidation of methanol on Pt electrode, *Journal of the American Chemical Society*, 13 (2003) 3680-3681.

[112] Xu, Xin, Guorui Yang, Jin Liang, Shujiang Ding, Chengli Tang, Honghui Yang, Wei Yan, Guidong Yang, and Demei Yu, Fabrication of one-dimensional heterostructured TiO 2@ SnO 2 with enhanced photocatalytic activity, *Journal of Materials Chemistry A* 2, no. 1 (2014) 116-122.

[113] Li, Xiaoxia, Aaron Li Zhu, Wei Qu, Haijiang Wang, Rob Hui, Lei Zhang, and Jiujun Zhang, Magneli phase Ti 4 O 7 electrode for oxygen reduction reaction and

its implication for zinc-air rechargeable batteries, *Electrochimica Acta*, 20 (2010) 5891-5898.

[114] Hahn, Robert, Felix Schmidt-Stein, Jarno Salonen, Stefan Thiemann, YanYan Song, Julia Kunze, Vesa-Pekka Lehto, and Patrik Schmuki, Semimetallic TiO2 *Angewandte* Nanotubes, *Chemie*, 39 (2009) 7372-7375.

[115] Di Valentin, Cristiana, Gianfranco Pacchioni, and Annabella Selloni, Theory of carbon doping of titanium dioxide, *Chemistry of Materials*, 26 (2005) 6656-6665.

[116] Walsh, F. C., and R. G. A. Wills, The continuing development of Magnéli phase titanium sub-oxides and Ebonex® electrodes, *Electrochimica Acta,* 22 (2010) 6342-6351.

[117] Li, Xingwei, Jiadi Wei, Yuzheng Chai, and Shuo Zhang,Carbon nanotubes/tin oxide nanocomposite-supported Pt catalysts for methanol electro-oxidation, *Journal of colloid and interface science,* 450 (2015) 74-81.

[118] Luo, Yong, Shirong Ge, Zhongmin Jin, and John Fisher,Formation of titanium carbide coating withámicro-porousástructure, *Applied Physics A*, 4 (2010) 765-768.

[119] Reyes-Garcia, Enrique A., Yanping Sun, Karla R. Reyes-Gil, and Daniel Raftery, Solid- state NMR and EPR analysis of carbon-doped titanium dioxide photocatalysts (TiO 2− xCx), *Solid state nuclear magnetic resonance*, 2 (2009) 74-81.

[120] Hahn, Robert, Andrei Ghicov, Jarno Salonen, Vesa-Pekka Lehto, and Patrik Schmuki, Carbon doping of self-organized TiO2 nanotube layers by thermal acetylene treatment, *Nanotechnology*, 10 (2007) 105604.

[121] W. Göpel, G. Rocker, R. Feierabend, Phys. Rev B, (1983) 283427–3438.

[122] Di Valentin, Cristiana, Gianfranco Pacchioni, and Annabella Selloni, Theory of carbon doping of titanium dioxide, *Chemistry of Materials*, 26 (2005): 6656-6665.